

LM-05K106
June 27, 2005

Neutron Capture and Total Cross Section Measurements and Resonance Parameters of Gadolinium

G Leinweber, DP Barry, MJ Trbovich, JA Burke, NJ Drindak,
HD Knox, RV Ballad, RC Block, Y Danon, LI Severnyak

NOTICE

This report was prepared as an account of work sponsored by the United States Government. Neither the United States, nor the United States Department of Energy, nor any of their employees, nor any of their contractors, subcontractors, or their employees, makes any warranty, express or implied, or assumes any legal liability or responsibility for the accuracy, completeness or usefulness of any information, apparatus, product or process disclosed, or represents that its use would not infringe privately owned rights.

Neutron Capture and Total Cross Section Measurements and Resonance Parameters of Gadolinium

G Leinweber, DP Barry, MJ Trbovich, JA Burke, NJ Drindak, HD Knox, and RV Ballad
Lockheed Martin Corporation, P.O. Box 1072, Schenectady, New York 12301-1072

RC Block, Y Danon, LI Severyak
*Rensselaer Polytechnic Institute, Department of Mechanical, Aerospace, and Nuclear
Engineering, Troy, New York 12180-3590*

July, 2005

Abstract- *Neutron capture and transmission measurements were performed by the time-of-flight technique at the Rensselaer Polytechnic Institute (RPI) linac facility using metallic and liquid Gd samples. The liquid samples were isotopically-enriched in either ^{155}Gd or ^{157}Gd . The capture measurements were made at the 25-m flight station with a multiplicity-type capture detector, and the transmission measurements were performed at 15- and 25-m flight stations with ^6Li glass scintillation detectors. The multilevel R-matrix Bayesian code SAMMY was used to extract resonance parameters.*

Among the significant findings are the following. The neutron width of the largest resonance in Gd, at 0.032 eV in ^{157}Gd , has been measured to be $(9\pm 1)\%$ smaller than that given in ENDF/B-VI updated through release 8. The thermal (2200 m/s) capture cross section of ^{157}Gd has been measured to be 11% smaller than that calculated from ENDF. The other major thermal resonance, at 0.025 eV in ^{155}Gd , did not display a significant deviation from the thermal capture cross section given by ENDF.

In the epithermal region, the analysis provided here represents the most extensive to date. Twenty eight new resonances are proposed and other resonances previously identified in the literature have been revisited. The assignment of resonances within regions of complicated structure incorporated the observations of other researchers, particularly on the six occasions where ENDF resonances are recommended to be removed. The poor match of the ENDF parameters to the current data is significant, and substantial improvement to the understanding of gadolinium cross sections is presented, particularly above 180 eV where the ENDF resolved region for ^{155}Gd ends.

I. Introduction

The purpose of the present work is to measure the neutron cross sections of gadolinium accurately. Gd has the highest thermal cross section of any natural element. Two large resonances exist slightly above thermal energy. The resonances are in ^{155}Gd and ^{157}Gd . Isotopically-enriched ^{155}Gd and ^{157}Gd samples were prepared as liquid solutions with heavy water to produce uniform, thin samples. These thin samples were used in conjunction with elemental, natural metal samples.

A more detailed description of the present measurement and analysis is given in Reference 1.

II. Historical Review

A review of the prior measurements of Gd shows that the resonance parameters for the low energy doublet (at ≈ 0.03 eV) in ENDF/B-VI² updated through release 8 are nearly identical to those of Møller et al.³ The neutron width of the low energy ^{155}Gd resonance and the radiation widths of both low energy resonances come directly from the paper of Møller et al.³, while the ENDF value for the neutron width of the low energy ^{157}Gd resonance is within 0.4% of the value given by Møller et al.³

In the region from 1.0 to 300.0 eV, most of the resonances occur in ^{155}Gd and ^{157}Gd . In these two isotopes, ENDF resonance parameters are based on a few experiments, particularly Mughabghab and Chrien⁴, Simpson⁵, and Fricke et al.⁶ The other high-abundance isotopes, ^{158}Gd and ^{160}Gd , have few resonances and their parameters come from Mughabghab and Chrien⁴ and Rahn et al.⁷ The minority isotopes are ^{152}Gd and ^{154}Gd . ^{152}Gd has a natural abundance of 0.2%. Its parameters come from Anufriev et al.⁸ and Macklin⁹. ^{154}Gd has a natural abundance of 2.1%. Its resonance parameters come from References 7 and 9.

Many other authors contributed observed resonance energies and/or spin assignments for resonances energies above 148 eV including Belyaev et al.¹⁰, Karshzhavina et al.^{11,12}, and Asghar et al.¹³.

III. Experimental Conditions

Table I gives some details of the experimental conditions including neutron targets, overlap filters, linac pulse repetition rate, flight path length, and channel widths. Descriptions of the detectors^{14,15}, data acquisition^{14,16}, and neutron-producing targets^{17,18,19} used in these experiments are available in the references.

The neutron energy for a detected event is determined using the time-of-flight (TOF) technique. The overall deadtime of the signal processing electronics has been set at 1.125 μs for capture measurements and 0.6 μs for transmission measurements.¹⁴

Table I**Gadolinium Experimental Details**

| Experiment | Overlap Filter | Neutron-Producing Target | Electron Pulse Width (ns) | Ave. Beam Curr. (μA) | Beam Energy (MeV) | Max Channel Width (μs) | Intermediate Channel Width (μs) | Min Channel Width (μs) | Pulse Repetition Rate (pulses/s) | Fl. Path L (m) |
|----------------------------------|----------------|--------------------------|---------------------------|----------------------|-------------------|------------------------|--------------------------------------|------------------------|----------------------------------|----------------|
| Epithermal Trans_a | Boron Carbide | Bare Bounce | 160 | 36 | 56 | 0.5 @ <27eV | 0.125 @ 27-236eV | 0.0625 @>236eV | 250 | 25 |
| Epithermal_Trans_b | Cadmium | Bare Bounce | 153 | 40 | 50 | 0.5 @ <27eV | 0.125 @ 27-236eV | 0.0625 @>236eV | 250 | 25 |
| Thermal_a Trans Enriched Liquids | None | Enhanced Thermal | 1000 | 8 | 53 | 128 @ <0.01 eV | 32 @0.01-0.04eV 8 @ 0.04-0.5eV | 0.5 @ >0.5 eV | 25 | 15 |
| Thermal_b Trans Enriched Liquids | None | Enhanced Thermal | 3000 | 19 | 60 | 256 @ <0.008 eV | 32 @ 0.008-0.04eV 8 @ 0.04-0.19eV | 1.0 @ >0.19 eV | 25 | 15 |
| Thermal_c Trans Natrl Metals | None | Enhanced Thermal | 2100 | 8.5 | 50 | 8 @ <0.29 eV | 1 @ 0.29-4.8 eV | 0.5 @>4.8eV | 25 | 15 |
| Epithermal Capture | Cadmium | Bare Bounce | 128 | 45 | 58 | 2 @ <1.5eV | 0.5 @ 1.5-27eV 0.125 @ 27-236eV | 0.0625 @>236eV | 250 | 25 |
| Thermal Capture | None | Enhanced Thermal | 3280 | 19 | 52 | 2048 @ <0.02 eV | 128 @ 0.02-0.06eV 16 @ 0.06-0.5eV | 1.0 @ >0.5 eV | 25 | 25 |

Table II lists the isotopic content of the gadolinium samples used in the experiments. The purity of metal samples was 99.8%. The isotopic abundances of the elemental metal samples are taken from Reference 20. The only significant contaminant in the metal samples was tantalum with a manufacturer-specified content of less than 0.1%. The liquid samples were prepared by dissolving enriched gadolinium oxide in D_2NO_3 , and then diluting in 99.80% pure D_2O . The uncertainties in isotopic enrichment of liquid samples given in Table II were determined by mass spectroscopy. No evidence of contamination was observed in the liquid sample data.

Table III lists the samples' thicknesses and the measurements made with these samples. The uncertainties in sample thickness for metal samples were propagated from multiple measurements of sample weight and diameter. The diameter measurements were the dominate component of the uncertainties. The uncertainties in sample thickness for liquid samples are larger than those of metals as shown in . The method used to determine the effective thickness of a liquid consists of weighing the quantity of Gd_2O_3 necessary for 10 ml of $GdNO_3$ solution in a 10 ml flask. Then, a known weight of DNO_3 is added to dissolve the Gd_2O_3 . Next, a known weight of D_2O is added to bring the volume to 10 ml. The concentration of Gd_2O_3 is the weight in grams divided by 10 ml. The weights are accurate to 0.001% for a 5 gram sample. The accuracy of this method is limited by the accuracy of the volumetric flask, 0.2%. Each of the samples used is a further dilution of the stock solution, introducing a second 0.2% error. Subsequent to the gadolinium sample preparation, a second method was developed. It consists of preparing more of each solution than is required, so that part of the batch can be extracted with a precision (0.02% of volume) pipette, fired and weighed. Experience has shown that estimates of sample thickness from these two methods can differ by 2%. The second method is preferred since it measures the final product. Application of this second method to the current measurements would require destructively analyzing the liquid samples used in this measurement which was not done. Therefore the uncertainty in sample thickness for the liquid samples is less than or equal to 2%.

All metal samples were natural elemental gadolinium sealed inside aluminum sample cans. The thickness of aluminum on each of the front and rear faces of each sample was 0.38 mm (15 mils; 1 mil = 0.001 in). The influence of these sample cans, as well as all background, was measured by including empty sample cans in the capture measurement. Background in transmission measurements is discussed in Section IV.B.

The liquid samples were enclosed in quartz cells. A drawing of the quartz cell is given in Figure 1. The liquid samples were needed to measure the strong thermal region doublet. The thinnest manufacturable metal sample of uniform thickness was 0.025 mm thick. At this thickness the thermal region doublet is saturated. The liquid samples provided a uniform solution of enriched Gd in heavy water. The heavy water minimized non-Gd interactions. The sample container was a quartz cell with parallel inner walls. A D_2O blank in an equivalent quartz container was included in the liquid sample measurements as a background measurement.

Table II Liquid Gadolinium Isotopic Enrichment, Atom Percentages

| | Samples | ^{152}Gd | ^{154}Gd | ^{155}Gd | ^{156}Gd | ^{157}Gd | ^{158}Gd | ^{160}Gd |
|------------------------------|--------------------------------|--------------------------|--------------------------|--------------------------|-------------------------|-------------------------|-------------------------|------------------------|
| ^{155}Gd - enriched | LX-1, LX-2, LX-4, LX-9 | 0.0108 ± 0.0002 | 0.9859 ± 0.0074 | 74.4233 ± 0.0095 | 17.5674 ± 0.0051 | 3.7513 ± 0.0023 | 2.5336 ± 0.0024 | 0.7278 ± 0.0020 |
| ^{157}Gd - enriched | LX-5, LX-6, LX-7, LX-10, LX-11 | 0.00510 ± 0.00004 | 0.07530 ± 0.00025 | 1.35147 ± 0.00070 | 7.3627 ± 0.0017 | 69.6623 ± 0.0081 | 19.4431 ± 0.0067 | 2.1000 ± 0.0015 |
| Elemental Metals | | 0.2 | 2.2 | 14.8 | 20.5 | 15.7 | 24.8 | 21.9 |

Table III Elemental Metals and Liquid Isotopic Samples

| Metal Samples | atoms/barn Gd | Uncertainty a/b Gd | Measurements Included |
|---------------------|---------------|-----------------------|--|
| 0.025 mm (0.001 in) | 9.119E-05 | 6E-08 | Thermal and epithermal transmission 0.024-10 eV, and capture 1-300 eV |
| 0.051 mm (0.002 in) | 1.713E-04 | 1E-07 | Thermal and epithermal transmission 0.055-10 eV, and capture 1-300 eV |
| 0.127 mm (0.005 in) | 4.127E-04 | 5E-07 | Thermal and epithermal transmission 0.088-300 eV, and capture 1-300 eV |
| 0.254 mm (0.010 in) | 7.806E-04 | 4E-07 | Epithermal transmission 10-300 eV |
| 0.508 mm (0.020 in) | 1.566E-03 | 5E-07 | Epithermal transmission 10-300 eV |
| 0.889 mm (0.035 in) | 2.886E-03 | 3E-06 | Epithermal transmission 10-300 eV |
| 1.27 mm (0.050 in) | 3.926E-03 | 2E-06 | Epithermal transmission 10-300 eV |
| 2.54 mm (0.100 in) | 8.070E-03 | 2.1E-05 | Epithermal transmission and capture 10-300 eV |
| 5.08 mm (0.200 in) | 1.577E-02 | 3E-05 | Epithermal transmission 10-300 eV |
| 1.02 cm (0.400 in) | 3.151E-02 | 6E-05 | Epithermal transmission 10-300 eV |
| Liquid Samples | atoms/barn Gd | Uncertainty a/b Gd | Measurements Included |
| LX-1 | 1.41E-04 | $\leq 2\%$ see Note 1 | Thermal transmission 0.047-1.0 eV |
| LX-2 | 4.58E-05 | $\leq 2\%$ see Note 1 | Thermal transmission 0.006-1.0 eV |
| LX-4 | 1.32E-05 | $\leq 2\%$ see Note 1 | Thermal transmission 0.002-1.0 eV, and thermal capture 0.01-1.0 eV |
| LX-5 | 1.27E-04 | $\leq 2\%$ see Note 1 | Thermal transmission 0.081-1.0 eV |
| LX-6 | 4.34E-05 | $\leq 2\%$ see Note 1 | Thermal transmission 0.046-1.0 eV |
| LX-7 | 1.19E-05 | $\leq 2\%$ see Note 1 | Thermal transmission 0.002-1.0 eV |
| LX-9 | 4.39E-06 | $\leq 2\%$ see Note 2 | Thermal capture 0.01-1.0 eV |
| LX-10 | 3.97E-06 | $\leq 2\%$ see Note 2 | Thermal capture 0.01-1.0 eV |
| LX-11 | 1.32E-06 | $\leq 2\%$ see Note 2 | Thermal capture 0.01-1.0 eV |

Note 1 – In the chemical preparation of the liquid samples, the uncertainty in sample thickness is limited by the two required measurements of volume, each with an estimated uncertainty of 0.2%. The quadrature sum error is $\sqrt{(2x^2)} \approx 0.3\%$. However, thicknesses determined in this manner have been found to be discrepant by 2% (see Section VII.A).

Note 2 – These three samples, LX-9, LX-10, and LX-11, were further diluted and therefore required a third measurement of volume with an uncertainty of 0.2%.

III.A. Capture Detector

The capture detector is a gamma detector containing 20 liters of NaI(Tl).^{14,15,16} The scintillation crystals form an annulus around the neutron beam with the sample at its center. The metal samples were 5.08 cm in diameter and the neutron beam was collimated to 4.76 cm. Neutrons that scatter from the sample are absorbed by a hollow cylindrical liner fabricated of boron carbide ceramic to reduce the number of scattered neutrons reaching the detector. The liner uses boron enriched to 98.4 w/o ^{10}B for maximum neutron absorption. The liquid samples were 1.27-cm in diameter and the neutron beam was collimated to 1.11 cm. The final collimator used for the liquid sample measurements was an annular cylinder of ^{10}B powder placed inside the detector just a few centimeters from the samples. The detector system discriminates against the 478 keV gamma ray from $^{10}\text{B}(\text{n},\alpha)$ reactions. The efficiency of the capture detector is assumed to be the same for all Gd isotopes. Reference 14 contains a description of the detector and its signal processing electronics.

III.B. Transmission Detectors

Neutron transmission measurements were conducted at the 15-meter and 25-meter flight stations. The 15-meter station contains a 7.62-cm (3-in) diameter, 0.3-cm-thick NE 905 ^6Li glass scintillation detector (6.6% lithium, enriched to 95% in ^6Li) and is used for measurements covering the energy range from 0.002 eV to 10 eV. The 25-meter station contains a 12.70-cm (5-in) diameter, 1.27-cm-thick NE 905 ^6Li glass detector and covers the range from 1 eV to 300 eV. Each detector is coupled to a photomultiplier tube.

Transmission samples along with empty sample holders, which are used to measure the open-beam count rate, are mounted on an 8-position computer-controlled sample changer. The transmission function, which is approximately the ratio of the count rate with a sample in the beam to the count rate with samples removed, varies with neutron energy. Each data run consists of one complete cycle through the samples, with a predetermined number of linac bursts for each sample position. The distribution of bursts per sample position is chosen to minimize the counting statistical error in the measured cross section.²¹

IV. Data Reduction

IV.A. Capture Data

Neutron capture data taking and data reduction techniques at the RPI linac are described in References 22 and 23.

For the thermal measurement of liquid samples, background was determined using a cell containing D_2O . For the epithermal measurement of metal samples, background was determined using empty aluminum sample cans.

Processed capture data are expressed as yield. Yield is defined as the number of neutron captures per neutron incident on the sample. Therefore, in addition to the sample data, another set of data was needed to determine the energy profile of the neutron flux. This was done by mounting a thick $^{10}\text{B}_4\text{C}$ sample in the sample changer and adjusting the total energy threshold to record the 478 keV gamma rays from neutron absorption in ^{10}B . The boron absorption spectrum provides an accurate representation of the energy profile of the linac's neutron beam flux convoluted with the $1/\nu$ boron (n,α) cross section. These flux data give the shape of the neutron beam flux, but not its magnitude. The thermal flux was smoothed using a cubic spline interpolation. The thermal yield was normalized to the transmission data in a combined SAMMY fit. The epithermal flux was normalized to the black 6.3-eV predominantly-capture resonance in Gd. A small correction (1.8%) was made for the scattering in the 6.3-eV normalizing resonance. The 2.54-mm (100-mil) sample data were used for this normalization.

The zero time for each experiment was determined by performing a 'gamma flash' measurement. The burst of gamma rays accompanying the neutron burst is detected by the capture detector. The centroid of the gamma-flash peak, less the time for light to travel the length of the flight path, is defined as the zero time of neutron production.

Finally, Y_i , the capture yield in time-of-flight channel i , was calculated by:

$$Y_i = \frac{C_i - B_i}{K\phi_i} \quad (1)$$

where C_i is the dead-time-corrected and monitor-normalized counting rate of the sample measurement,
 B_i is the dead-time-corrected and monitor-normalized background counting rate,
 K is the product of the flux normalization factor and efficiency, and
 Φ_i is the unnormalized neutron flux.

It was this capture yield and its associated statistical uncertainty that provided input to the SAMMY²⁴ data analysis code that extracted the neutron resonance parameters.

Four liquid capture samples were used in the analysis of the thermal region. The low energy cutoff for capture data in the thermal region was 0.01 eV. Four natural metal samples were used in the epithermal region, 1-300 eV.

The flux-to-background ratio in the liquid sample thermal capture experiment peaked at approximately 35-to-1 at 0.1 eV, is 20-to-1 at the thermal region doublet, and fell to 3-to-1 at 0.01 eV. Capture data were not used below 0.01 eV. The flux-to-background ratio for the natural metal epithermal capture experiment was approximately

400-to-1 from 150-300 eV, and fell steadily to 300-to-1 at 40 eV, to 200-to-1 at 10 eV, and 80-to-1 at 2 eV.

IV.B. Transmission Data

For the thermal measurement, liquid sample cells containing D₂O were used as the open beam measurement. In this way the effect of the D₂O and quartz in the sample and open cells would cancel in transmission.

The time-dependent background was obtained with the one-notch/two-notch method.²⁵ The transmission function was calculated from equation (2).

$$T_i = \frac{(C_i^S - K_S B_i - B_S)}{(C_i^O - K_O B_i - B_O)} \quad (2)$$

where

T_i , the transmission in time-of-flight channel i,

C_i^S and C_i^O are the dead-time corrected and monitor-normalized counting rates of the sample and open measurements, respectively,

B_i is the time-dependent background counting rate,

B_S and B_O are the steady state background counting rates for sample and open measurements, respectively, and

K_S and K_O are the normalization factors for the sample and open background measurements.

The two thermal liquid sample measurements' backgrounds were normalized to extrapolated notch data in Cd at 0.15 eV.

Correction factors of up to 1.3% were applied to LX-1, 5, and 6 thermal transmission data due to sample misalignment, so that their transmissions went to zero in the saturated low-energy region.

For the thermal metal measurement, a single exponential function was used to interpolate between two known background points: a fixed indium notch at 1.4 eV and the region below 0.01 eV, where all metal Gd samples are black. Normalization constants K_S and K_O were fixed at 1.0 for the thermal metal measurement. Each sample's background function was calculated individually.

The first epithermal measurement's background was normalized to the extrapolated notch in silver at 5.2 eV for all samples except the 1.02-cm (400-mil) sample, which was normalized at the saturated 20.5 eV resonance in Gd.

The second epithermal measurement's background was normalized to the extrapolated notch in tungsten at 18.8 eV.

The epithermal flight path length (\approx 25.6 m) and zero time were fitted to match the energies from epithermal capture data.

Seven liquid transmission data sets were used in the thermal analysis. Three natural metal samples were used in the thermal and epithermal energy ranges up to 10 eV. Eleven additional natural metal transmission data sets were used in the epithermal analysis from 1 – 300 eV.

The signal-to-background ratios for the two liquid sample thermal experiments peaked at 2000-to-1 near 0.5 eV. The ratio in the region of the two strong thermal resonances in Gd was 1000-to-1. Signal-to-background fell to 10-to-1 at 2 meV, the lowest energy at which data were used. Signal-to-background ratios for the metal sample thermal experiment was 1000-to-1 or greater from thermal energies through 0.1 eV with a peak value of 2000-to-1 at 0.06 eV. The ratio fell to 200-to-1 at 0.5 eV and remained steady at 200-to-1 out to 10 eV. Signal-to-background ratios for the two metal sample epithermal experiments were rather constant with energy at approximately 45-to-1 for the boron-filtered experiment and approximately 75-to-1 for the cadmium-filtered experiment.

V. Analysis Methods

Resonance parameters, neutron width, Γ_n , radiation width, Γ_γ , and resonance energy, E_0 , were extracted from the capture and transmission data sets using the multi-level R-matrix Bayesian code SAMMY version M6.²⁴ This was a combined transmission and capture analysis, which employed the resolution broadening, self-shielding, multiple-scattering, and diluent features of SAMMY. The present measurements assumed the same spin assignments as ENDF for all resonances analyzed.

In the liquid thermal capture measurement a D₂O-only “blank” cell was used to measure background. The data were processed by subtracting the blank from the Gd plus D₂O capture data. The SAMMY geometry consists of a homogeneous mixture of Gd and D₂O. The three-dimensional geometry in MCNP²⁶ allowed a realistic treatment of the neutron scattering and capture in Gd, D₂O, and the quartz cells. The resulting correction factors were applied to the liquid capture yield data. The factors ranged from 1.02 at 0.01 eV to 0.995 at 0.1 eV. They accounted primarily for quartz scattering and subsequent capture in Gd, which could not be modeled in SAMMY. More details are provided in Reference 1.

For liquid thermal transmission analysis, no diluent, i.e. D₂O, specifications are needed. That is because D₂O-only “blank” cells are used for the open beam measurement and therefore the effect of the diluent cancels experimentally from the transmission,

defined as (quartz + sample + diluent) / (quartz + diluent-only open beam). Therefore, the SAMMY model includes only Gd. The presence of Gd in the samples is so dilute that there is no need to account for D₂O displaced by the Gd.

The following assumptions were made for the SAMMY analysis:

- Background was not fitted during the SAMMY analysis which determined the final resonance parameters. Background was only varied in transmission in the 10-80 eV region as a sensitivity study for the purpose of determining uncertainties.
- Resonance parameters of the two bound level resonances of Gd (¹⁵²Gd and ¹⁵⁴Gd) were not varied.
- Resonance parameters of ¹⁵²Gd were not varied due to its low abundance (0.2%). They were fixed to ENDF values.
- Normalization of the liquid sample thermal capture data was varied within a combined capture and transmission SAMMY fit.
- Normalization was not varied for either capture or transmission in the epithermal region.
- Energy regions over which each sample has been fitted are given in Table III. Low energy cutoffs were chosen at a point where transmission falls below 1%. The thermal flux peaks at \approx 0.08 eV and drops off rapidly with decreasing energy. The combination of low flux and the highly absorbing nature of gadolinium at subthermal energies led to regions of low transmission where the accuracy of the background treatment is important.
- There were concerns about background in both epithermal transmission measurements using metal samples below 80 eV, and particularly below 10 eV. Therefore, the low-energy cut-off for these data sets was 10 eV.

The potential scattering lengths used in the present analysis for gadolinium are taken from ENDF. The potential scattering lengths used for deuterium and oxygen in the liquid samples were 5.20 fm and 5.46 fm, respectively. These radii were calculated from potential scattering cross-sections, deuterium $\sigma_s = 3.4$ barns, oxygen $\sigma_s = 3.75$ barns.²⁷

The potential scattering lengths for each of the gadolinium isotopes except ¹⁵²Gd were varied with SAMMY to obtain a better fit to the thick (5.08-mm) transmission data. The resulting potential scattering lengths were similar to ENDF, ± 0.1 ;.

The radius to be used for penetrabilities and shifts were calculated using equation (3).⁸

$$a = 1.23 * AWRI^{1/3} + 0.8 \quad (3)$$

where,

a is the channel radius, and

$AWRI$ is the atomic weight given in the ENDF file. This atomic weight is based on the mass of the neutron rather than amu.

The effective temperature was 293 K, and no external R-function was employed. Distant resonances were represented by including all of the resonances present in the ENDF file. No p-wave resonances were observed in the energy range currently being reported.

The manufacturer-specified tantalum content of the natural metal samples was 0.1%. A SAMMY fit of thick samples to the strong 4.28 eV resonance in tantalum yielded an abundance of 0.13% which was used in all resonance parameter fits. That is, all ENDF resonances for Ta were included in all metal-sample SAMMY calculations with an abundance of 0.13%.

Resonance integrals are defined in equation (4).

$$RI = \int_{0.5eV}^{\infty} \sigma_c(E) \frac{dE}{E} \quad (4)$$

where RI is the infinitely dilute capture resonance integral, in barns, and $\sigma_c(E)$ is the neutron capture cross section in barns

Resonance integrals and thermal cross sections were calculated using the NJOY²⁸ program. The resonance integrals were evaluated from 0.5 eV to 20 MeV. One calculation was performed using ENDF resonance parameters and one calculation was performed with RPI resonance parameters replacing the ENDF parameters for all resonances below 300 eV. Results are presented in Section VI.C.

VI. Results

VI.A Results- Thermal

Resonance parameters were determined in a covariance-matrix-linked SAMMY calculation. The resulting resonance parameters for the two thermal region resonances are given in Table IV. ENDF/B-VI resonance parameters are nearly identical to those of Möller et al.³ The uncertainties given in Reference 3 are reported as ENDF uncertainties in Table IV. The uncertainties given in Table IV for the thermal region were estimated to be on the order of 1σ and include the following considerations: internal consistency of the transmission data, reproducibility of transmission results, the uncertainty in capture flux normalization, and the balance of interactions between the overlapping ^{155}Gd and ^{157}Gd thermal resonances.

Table IV Thermal Results: Resonance Parameters

| Dataset | Energy, eV | Γ_γ , meV | Γ_n , meV | ISOTOPE | J |
|-----------|---------------------|-----------------------|---------------------|---------|---|
| ENDF-B/VI | 0.0268 ± 0.0002 | 108 ± 1 | 0.104 ± 0.002 | 155 | 2 |
| | 0.0314 ± 0.0002 | 106 ± 1 | 0.4704 ± 0.0080 | 157 | 2 |
| RPI | 0.025 ± 0.003 | 104 ± 3 | 0.097 ± 0.003 | 155 | 2 |
| | 0.032 ± 0.003 | 107 ± 3 | 0.428 ± 0.004 | 157 | 2 |

The methods used to estimate the RPI uncertainties are discussed in Section VII and Reference 1. Since both of these resonances are predominantly capture resonances, both transmission and capture measurements were essentially measuring capture. Neutron width is the resonance parameter that was most sensitive to the data in both capture and transmission. The neutron widths for both resonances were found to be smaller than ENDF, by 9% in the ^{157}Gd resonance and by 7% in the smaller ^{155}Gd resonance.

Fourteen samples were included in this calculation: seven liquid transmission samples (4 enriched in ^{155}Gd , 3 enriched in ^{157}Gd), three natural metal transmission samples, and four liquid capture samples (2 enriched in ^{155}Gd , 2 enriched in ^{157}Gd). No natural metal capture measurements were made. An overview of the data and the SAMMY calculations using RPI resonance parameters is shown in **Figure 2**. Comparisons of some of the present results to ENDF are shown in **Figure 3**. The inability of a single set of resonance parameters to fit all data sets simultaneously is due to internal inconsistencies in the data. The SAMMY fit was a statistically-weighted combination of the data sets. Each sample's name and the isotope that it's enriched in is given in the legends of each figure. The isotopic content in each sample is given in Table II. The thermal-region ^{157}Gd resonance is approximately four times stronger than the ^{155}Gd resonance and their relative abundances in natural metal are approximately the same (see Table II).

The ^{157}Gd neutron width is determined predominantly from natural metal transmission data and ^{157}Gd -enriched liquid sample transmission data. Capture normalization, in turn, is determined predominantly by the transmission-derived ^{157}Gd neutron width. The ^{155}Gd neutron width is determined predominantly by ^{155}Gd -enriched liquid transmission data, and to a lesser extent, by natural metal transmission data and ^{155}Gd -enriched liquid sample capture data. In the present data, transmission data have smaller statistical uncertainties than capture yield data, and thick samples have more influence on derived resonance parameters than thin samples in both capture and transmission.²¹

VI.B Results- Epithermal

An overview of the SAMMY fit in the epithermal region is given in Figure 4. The epithermal region was analyzed in two parts. First the 1-10 eV region was fitted with a combination of thermal transmission and epithermal capture data sets (see Section V). Second, the 10-300 eV region was fitted using data entirely from natural metal samples in capture and transmission. Resonance parameters for the epithermal region are given in Table V. The uncertainties quoted in Table V for the epithermal region were estimated to be on the order of 1σ , are described in Section VII and Reference 1, and include the following considerations: Consistency between capture and transmission results, stability of radiation widths, uncertainty in transmission background treatment, and Bayesian statistical errors. There are 28 new resonances introduced that were not included in ENDF. Six resonances present in ENDF have been discarded because the literature does not demonstrate their existence nor do the present measurements support their existence. Parameters for several resonances, particularly those from ^{152}Gd , were not fitted because the resonances were very weak. In these cases the resonance parameters are assigned ENDF values and are listed in Table V without any quoted errors.

VI.B.1 Results- Epithermal; The 1-10 eV region

Resonance parameters resulting from the SAMMY fit are given in Table V. The same three samples were measured in both transmission and capture, i.e., 0.025 mm (1 mil), 0.051 mm (2 mil), and 0.127 mm (5 mil) natural metal Gd. The radiation width for the weak 3.6 eV resonance in ^{155}Gd was not varied from ENDF values.

VI.B.2 Results- Epithermal; The 10-300 eV region

Fifteen data sets were used in the region above 10 eV. There were two separate transmission measurements. The first used a B_4C overlap filter and included samples of the following thicknesses: 0.127 mm (5 mil), 0.254 mm (10 mil), 0.508 mm (20 mil), 0.889 mm (35 mil), and 1.27 mm (50 mil). The second epithermal transmission measurement used a Cd overlap filter and included samples of the following thicknesses: 0.508 mm (20 mil), 0.889 mm (35 mil), 1.27 mm (50 mil), 2.54 mm (100 mil), 5.08 mm (200 mil), and 1.02 cm (400 mil). The capture measurement used a Cd overlap filter and included samples of the following thicknesses: 0.025 mm (1 mil), 0.051 mm (2 mil), 0.127 mm (5 mil), and 2.54 mm (100 mil).

Table V Epithermal Results: Resonance Parameters

| Energy eV | Energy ENDF meV | Γ_Y meV | Γ_Y ENDF meV | Γ_n ($2\alpha g\Gamma_n$ for unassigned) meV | Γ_n ENDF meV | ISO- TOPE ENDF | J ENDF |
|---------------------|-----------------------|-------------------|---------------------------|---|---------------------------|----------------------|---------------|
| 2.0120 \pm 0.0002 | 2.008 | 128 \pm 1 | 110.00 | 0.40 \pm 0.01 | 0.371 | 155 | 1 |
| 2.5729 \pm 0.0003 | 2.568 | 107.1 \pm 0.4 | 111.00 | 1.706 \pm 0.003 | 1.744 | 155 | 2 |
| 2.8287 \pm 0.0003 | 2.825 | 109.7 \pm 0.9 | 97.00 | 0.377 \pm 0.004 | 0.345 | 157 | 2 |
| 3.616 \pm 0.003 | 3.616 | 130 | 130.00 | 0.05 \pm 0.02 | 0.044 | 155 | 1 |
| 6.3057 \pm 0.0002 | 6.300 | 108.8 \pm 0.6 | 114.00 | 2.20 \pm 0.01 | 2.000 | 155 | 2 |
| 7.7477 \pm 0.0004 | 7.750 | 109 \pm 1 | 124.00 | 1.16 \pm 0.01 | 1.120 | 155 | 2 |
| 9.991 \pm 0.003 | 10.010 | 110 \pm 20 | 115.00 | 0.20 \pm 0.04 | 0.168 | 155 | 2 |
| 11.508 \pm 0.001 | 11.530 | 120 \pm 40 | 125.00 | 0.78 \pm 0.08 | 0.600 | 155 | 1 |
| 11.57 \pm 0.05 | 11.580 | 90 \pm 80 | 88.00 | 0.2 \pm 0.2 | 0.350 | 154 | $\frac{1}{2}$ |
| 11.964 \pm 0.008 | 11.990 | 130 \pm 20 | 112.00 | 1.12 \pm 0.04 | 0.880 | 155 | 2 |
| 12.35 | 12.350 | 58.6 | 58.60 | 4.65 | 4.650 | 152 | $\frac{1}{2}$ |
| 14.476 \pm 0.009 | 14.510 | 130 \pm 10 | 103.00 | 3.43 \pm 0.09 | 3.200 | 155 | 1 |
| 16.201 \pm 0.005 | 16.240 | 130 \pm 30 | 91.00 | 0.44 \pm 0.03 | 0.400 | 157 | 1 |
| 16.78 \pm 0.01 | 16.770 | 112 \pm 7 | 80.50 | 13.9 \pm 0.5 | 12.800 | 157 | 2 |
| 17.729 \pm 0.005 | 17.770 | 130 \pm 40 | 120.00 | 0.47 \pm 0.04 | 0.392 | 155 | 2 |
| 19.86 \pm 0.01 | 19.920 | 118 \pm 6 | 104.00 | 4.5 \pm 0.1 | 4.560 | 155 | 2 |
| 20.51 \pm 0.02 | 20.560 | 106 \pm 8 | 88.00 | 13.4 \pm 0.4 | 11.360 | 157 | 2 |
| 20.97 \pm 0.02 | 21.030 | 140 \pm 20 | 98.00 | 11.6 \pm 0.5 | 15.600 | 155 | 2 |
| 21.59 \pm 0.02 | 21.650 | 80 \pm 40 | 114.00 | 0.34 \pm 0.08 | 0.376 | 157 | 2 |
| 22.30 \pm 0.04 | 22.300 | 100 \pm 40 | 96.00 | 7.1 \pm 0.8 | 6.000 | 158 | $\frac{1}{2}$ |
| 22.5 \pm 0.2 | 22.330 | 100 \pm 100 | 88.00 | 20 \pm 10 | 11.500 | 154 | $\frac{1}{2}$ |
| 23.28 \pm 0.03 | 23.330 | 140 \pm 30 | 121.00 | 1.3 \pm 0.3 | 0.813 | 157 | 1 |
| 23.60 \pm 0.02 | 23.670 | 140 \pm 10 | 120.00 | 2.91 \pm 0.08 | 3.120 | 155 | 2 |
| 25.35 \pm 0.01 | 25.400 | 130 \pm 30 | 85.00 | 1.99 \pm 0.06 | 1.840 | 157 | 2 |
| 27.509 \pm 0.002 | 27.570 | 140 \pm 20 | 125.00 | 1.31 \pm 0.04 | 1.120 | 155 | 1 |
| 29.50 \pm 0.02 | 29.580 | 113 \pm 2 | 108.00 | 4.8 \pm 0.1 | 4.320 | 155 | 2 |
| 30.05 \pm 0.02 | 30.100 | 130 \pm 10 | 100.00 | 11.1 \pm 0.5 | 10.400 | 155 | 2 |
| 31.66 \pm 0.01 | 31.720 | 140 \pm 20 | 118.00 | 1.24 \pm 0.07 | 1.120 | 155 | 2 |
| 33.1 \pm 0.2 | 33.140 | 110 \pm 30 | 109.80 | 1.6 \pm 0.6 | 1.867 | 155 | 1 |
| 33.14 \pm 0.03 | 33.230 | 98 \pm 3 | 90.00 | 14 \pm 2 | 14.600 | 156 | $\frac{1}{2}$ |
| 33.4 \pm 0.3 | 33.510 | 120 \pm 90 | 115.00 | 1 \pm 4 | 1.600 | 155 | 1 |
| 34.73 \pm 0.02 | 34.830 | 131 \pm 4 | 152.00 | 6.8 \pm 0.2 | 6.133 | 155 | 1 |
| 35.39 \pm 0.01 | 35.470 | 140 \pm 10 | 118.00 | 2.17 \pm 0.06 | 1.840 | 155 | 2 |
| 36.86 | 36.860 | 56 | 56.00 | 84 | 84.000 | 152 | $\frac{1}{2}$ |
| 37.066 \pm 0.003 | 37.120 | 139 \pm 6 | 101.00 | 8.3 \pm 0.3 | 8.400 | 155 | 1 |
| 38.93 \pm 0.01 | 39.000 | 130 \pm 60 | 118.00 | 1.25 \pm 0.07 | 1.040 | 155 | 2 |
| 39.30 | 39.300 | 56 | 56.00 | 39 | 39.000 | 152 | $\frac{1}{2}$ |
| 40.08 \pm 0.01 | 40.170 | 120 \pm 40 | 110.00 | 1.6 \pm 0.2 | 1.307 | 157 | 1 |
| 42.73 | 42.730 | 56 | 56.00 | 3.06 | 3.060 | 152 | $\frac{1}{2}$ |
| 43.83 \pm 0.07 | 43.920 | 140 \pm 90 | 136.00 | 18 \pm 9 | 17.333 | 155 | 1 |
| 44.11 \pm 0.04 | 44.220 | 120 \pm 70 | 96.00 | 9 \pm 5 | 8.960 | 157 | 2 |
| 45.98 \pm 0.02 | 46.100 | 128 \pm 6 | 126.00 | 2.3 \pm 0.1 | 2.240 | 155 | 2 |
| 46.79 \pm 0.02 | 46.870 | 140 \pm 30 | 100.00 | 10.2 \pm 0.4 | 5.360 | 155 | 2 |
| 47.18 \pm 0.04 | 47.070 | 89 \pm 8 | 88.00 | 2.4 \pm 0.6 | 3.200 | 154 | $\frac{1}{2}$ |
| 47.628 \pm 0.006 | 47.730 | 107 \pm 10 | 109.80 | 0.39 \pm 0.03 | 0.653 | 155 | 1 |
| 48.68 \pm 0.03 | 48.790 | 118 \pm 9 | 90.00 | 26.7 \pm 0.5 | 24.000 | 157 | 2 |
| 49.63 \pm 0.07 | 49.500 | 90 \pm 40 | 88.00 | 3 \pm 1 | 1.800 | 154 | $\frac{1}{2}$ |
| 51.25 \pm 0.03 | 51.380 | 130 \pm 30 | 109.80 | 20.3 \pm 0.6 | 18.667 | 155 | 1 |
| 52.01 \pm 0.03 | 52.130 | 140 \pm 20 | 115.00 | 20.9 \pm 0.8 | 19.467 | 155 | 1 |

Table V (continued) Epithermal Results: Resonance Parameters

| Energy eV | Energy | | Γ_γ | | Γ_n | | Γ_n | ISO- |
|--------------------|-------------|------|-----------------|--------|------------------------------------|-------------|--------------|---------------|
| | ENDF meV | meV | ENDF meV | meV | (2ag Γ_n for unassigned) | ENDF meV | TOPE ENDF | J ENDF |
| 52.89 \pm 0.02 | 53.030 | 80 | \pm 30 | 109.80 | 1.2 \pm 0.2 | 1.360 | 155 | 2 |
| 53.62 \pm 0.02 | 53.740 | 140 | \pm 30 | 92.00 | 8.7 \pm 0.2 | 7.680 | 155 | 2 |
| 56.12 \pm 0.01 | 56.220 | 120 | \pm 40 | 120.00 | 2.5 \pm 0.1 | 2.160 | 155 | 2 |
| 58.26 \pm 0.03 | 58.300 | 140 | \pm 20 | 101.00 | 32.0 \pm 0.6 | 28.000 | 157 | 2 |
| 59.30 \pm 0.01 | 59.320 | 140 | \pm 40 | 129.00 | 6.9 \pm 0.4 | 6.640 | 155 | 2 |
| 62.73 \pm 0.02 | 62.840 | 150 | \pm 30 | 90.00 | 8.5 \pm 0.5 | 8.000 | 155 | 2 |
| 64.028 \pm 0.006 | 64.090 | 110 | \pm 40 | 109.80 | 0.49 \pm 0.05 | 0.256 | 155 | 2 |
| 65.21 \pm 0.01 | 65.060 | 100 | \pm 20 | 57.00 | 32 \pm 5 | 24.000 | 154 | $\frac{1}{2}$ |
| 66.4 \pm 0.5 | 65.200 | 120 | \pm 10 | 109.80 | 0.5 \pm 0.4 | 1.333 | 155 | 1 |
| 66.53 \pm 0.01 | 66.560 | 130 | \pm 60 | 67.00 | 16 \pm 2 | 14.667 | 157 | 1 |
| 69.4 \pm 0.1 | 69.400 | 100 | \pm 100 | 109.80 | 12 \pm 4 | 6.320 | 155 | 2 |
| 74.34 | 74.340 | 50.4 | | 50.40 | 60 | 60.000 | 152 | $\frac{1}{2}$ |
| 76.00 \pm 0.03 | 76.120 | 90 | \pm 50 | 88.00 | 2.0 \pm 0.9 | 1.100 | 154 | $\frac{1}{2}$ |
| 76.85 \pm 0.01 | 77.000 | 110 | \pm 60 | 109.80 | 3.0 \pm 0.3 | 1.600 | 155 | 2 |
| 77.63 \pm 0.01 | 77.800 | 110 | \pm 20 | 109.80 | 0.9 \pm 0.1 | 1.200 | 155 | 1 |
| 78.75 \pm 0.06 | 78.800 | 110 | \pm 30 | 109.80 | 8 \pm 1 | 4.240 | 155 | 2 |
| 80.04 \pm 0.07 | 80.200 | 80 | \pm 7 | 86.00 | 80 \pm 20 | 50.900 | 156 | $\frac{1}{2}$ |
| 80 | 80.050 | 112 | \pm 4 | 109.80 | 0 \pm 3 | 0.312 | 155 | 2 |
| 80.9 \pm 0.3 | 80.900 | 110 | \pm 30 | 109.80 | 1.44 \pm 0.09 | 2.400 | 155 | 1 |
| 81.30 \pm 0.04 | 81.480 | 110 | \pm 40 | 108.00 | 24 \pm 2 | 20.000 | 157 | 1 |
| 82.10 \pm 0.04 | 82.240 | 100 | \pm 70 | 99.95 | 7.1 \pm 0.6 | 6.160 | 157 | 2 |
| 83.97 \pm 0.02 | 84.200 | 120 | \pm 40 | 109.80 | 10.3 \pm 0.1 | 9.200 | 155 | 1 |
| 84.91 \pm 0.01 | 85.000 | 110 | \pm 40 | 109.80 | 2.2 \pm 0.3 | 3.067 | 155 | 1 |
| 85.55 | 85.550 | 58.6 | | 58.60 | 5.11 | 5.110 | 152 | $\frac{1}{2}$ |
| 87.17 \pm 0.03 | 87.210 | 140 | \pm 10 | 128.00 | 11.1 \pm 0.4 | 10.160 | 157 | 2 |
| 90.51 \pm 0.02 | 90.500 | 110 | \pm 90 | 109.80 | 2.5 \pm 0.2 | 1.280 | 155 | 2 |
| 92.40 | 92.400 | 58.6 | | 58.60 | 142 | 142.000 | 152 | $\frac{1}{2}$ |
| 92.47 \pm 0.02 | 92.500 | 110 | \pm 20 | 109.80 | 2.14 \pm 0.06 | 2.160 | 155 | 2 |
| 92.90 \pm 0.03 | 92.800 | 110 | \pm 50 | 109.80 | 3.48 \pm 0.07 | 3.120 | 155 | 2 |
| 93.99 \pm 0.01 | 94.100 | 110 | \pm 40 | 109.80 | 0.64 \pm 0.09 | 0.544 | 155 | 2 |
| 95.70 \pm 0.03 | 95.700 | 110 | \pm 50 | 109.80 | 7.1 \pm 0.4 | 3.840 | 155 | 2 |
| 96.4 \pm 0.2 | 96.600 | 110 | \pm 50 | 109.80 | 3.8 \pm 0.7 | 6.267 | 155 | 1 |
| 96.6 \pm 0.1 | 96.520 | 100 | \pm 40 | 110.00 | 22.0 \pm 0.4 | 12.160 | 157 | 2 |
| 98.30 \pm 0.03 | 98.300 | 150 | \pm 20 | 109.80 | 11.7 \pm 0.4 | 17.333 | 155 | 1 |
| 99.9 \pm 0.1 | 100.200 | 110 | \pm 10 | 109.80 | 2.5 \pm 0.2 | 2.133 | 155 | 1 |
| 100.16 \pm 0.06 | 100.200 | 100 | \pm 30 | 94.00 | 43 \pm 1 | 46.667 | 157 | 1 |
| 100.72 \pm 0.08 | 100.700 | 90 | \pm 40 | 82.00 | 48 \pm 7 | 32.000 | 154 | $\frac{1}{2}$ |
| 101.20 \pm 0.09 | 101.100 | 120 | \pm 10 | 105.00 | 1.3 \pm 0.2 | 1.000 | 158 | $\frac{1}{2}$ |
| 101.42 \pm 0.02 | 101.400 | 140 | \pm 30 | 109.80 | 2.1 \pm 0.2 | 2.720 | 155 | 2 |
| 102.03 \pm 0.03 | 102.100 | 110 | \pm 50 | 109.80 | 1.52 \pm 0.06 | 1.733 | 155 | 1 |
| 104.36 \pm 0.09 | 104.400 | 110 | \pm 80 | 109.80 | 5 \pm 1 | 9.067 | 155 | 1 |
| 104.89 \pm 0.08 | 104.950 | 103 | \pm 2 | 70.00 | 70 \pm 40 | 57.333 | 157 | 1 |
| 105.8 \pm 0.1 | 105.900 | 140 | \pm 20 | 109.80 | 6 \pm 1 | 6.133 | 155 | 1 |
| 106.05 \pm 0.08 | 105.600 | 110 | \pm 20 | 88.00 | 11 \pm 2 | 4.800 | 154 | $\frac{1}{2}$ |
| 107.14 \pm 0.04 | 107.100 | 110 | \pm 80 | 109.80 | 9 \pm 2 | 6.240 | 155 | 2 |
| 107.46 \pm 0.06 | 107.460 | 120 | \pm 30 | 99.95 | 4 \pm 1 | 5.600 | 157 | 2 |
| 109.37 \pm 0.02 | 109.600 | 115 | \pm 2 | 109.80 | 7.3 \pm 0.5 | 4.667 | 155 | 1 |
| 110.54 \pm 0.07 | 110.460 | 140 | \pm 50 | 85.00 | 50 \pm 20 | 42.400 | 157 | 2 |
| 112.40 \pm 0.04 | 112.400 | 90 | \pm 70 | 84.00 | 9.1 \pm 0.2 | 9.040 | 155 | 2 |
| 113.81 \pm 0.05 | 113.800 | 130 | \pm 20 | 67.00 | 20 \pm 1 | 15.200 | 155 | 2 |
| 115.37 \pm 0.06 | 115.350 | 140 | \pm 20 | 112.00 | 22.2 \pm 0.9 | 19.200 | 157 | 2 |

Table V (continued) Epithermal Results: Resonance Parameters

| Energy eV | Energy | | Γ_γ | | Γ_n | | Γ_n | | ISO- | | J ENDF |
|-------------------|------------|---------|-----------------|--------|-------------|------------------------------------|-------------|------------|---------------|--------------|-----------|
| | ENDF eV | meV | ENDF meV | meV | ENDF meV | (2ag Γ_n for unassigned) | ENDF meV | meV | ENDF | TOPE ENDF | |
| 116.56 \pm 0.06 | 116.500 | 120 | \pm 80 | 116.00 | 21 | \pm 1 | 17.333 | 155 | 1 | | |
| 118.66 \pm 0.02 | 118.600 | 110 | \pm 50 | 109.80 | 2.5 | \pm 0.4 | 2.000 | 155 | 2 | | |
| 120.83 \pm 0.01 | 121.000 | 130 | \pm 30 | 91.00 | 140 | \pm 40 | 132.000 | 157 | 2 | | |
| 123.35 \pm 0.05 | 123.400 | 200 | \pm 100 | 159.00 | 40 | \pm 6 | 36.000 | 155 | 1 | | |
| 124.25 \pm 0.08 | 124.000 | 110 | \pm 50 | 85.00 | 150 | \pm 20 | 124.000 | 154 | $\frac{1}{2}$ | | |
| 124.49 \pm 0.03 | 124.400 | 120 | \pm 20 | 109.80 | 4 | \pm 1 | 6.640 | 155 | 2 | | |
| 126.11 \pm 0.02 | 126.000 | 110 | \pm 60 | 109.80 | 14.6 | \pm 0.4 | 20.533 | 155 | 1 | | |
| 128.53 \pm 0.02 | 128.600 | 110 | \pm 30 | 109.80 | 1.7 | \pm 0.2 | 1.120 | 155 | 2 | | |
| 129.82 \pm 0.01 | 129.800 | 110 | \pm 40 | 109.80 | 3.4 | \pm 0.3 | 2.560 | 155 | 2 | | |
| 130.79 \pm 0.01 | 130.800 | 150 | \pm 30 | 109.80 | 22 | \pm 3 | 48.533 | 155 | 1 | | |
| 131.37 \pm 0.01 | NEW | 130 | \pm 10 | NEW | 1.27 | \pm 0.08 | NEW | UNASSIGNED | | | |
| 133.04 \pm 0.01 | 133.000 | 140 | \pm 20 | 109.80 | 5.3 | \pm 0.4 | 3.733 | 155 | 1 | | |
| 133.95 \pm 0.01 | 133.800 | 110 | \pm 30 | 109.80 | 3.4 | \pm 0.2 | 2.320 | 155 | 2 | | |
| 135.13 \pm 0.02 | 134.700 | 110 | \pm 60 | 109.80 | 1.9 | \pm 0.1 | 0.880 | 155 | 2 | | |
| DISCARDED | | 135.100 | | 99.95 | | | 0.880 | 157 | 2 | | |
| DISCARDED | | 137.900 | | 99.95 | | | 78.667 | 157 | 1 | | |
| 137.99 \pm 0.08 | 137.800 | 120 | \pm 80 | 109.80 | 90 | \pm 30 | 21.333 | 155 | 1 | | |
| 138.2 \pm 0.2 | 138.700 | 100 | \pm 10 | 86.00 | 21 | \pm 9 | 82.667 | 157 | 1 | | |
| 138.9 \pm 0.2 | 139.200 | 94 | \pm 8 | 91.00 | 40 | \pm 10 | 124.000 | 154 | $\frac{1}{2}$ | | |
| 139.37 \pm 0.05 | 139.300 | 100 | \pm 70 | 99.95 | 40 | \pm 10 | 10.000 | 157 | 1 | | |
| 140.00 | 140.000 | 58.6 | | 58.60 | 78.8 | | 78.800 | 152 | $\frac{1}{2}$ | | |
| 140.55 \pm 0.05 | 140.400 | 130 | \pm 10 | 109.80 | 4.9 | \pm 0.3 | 4.133 | 155 | 1 | | |
| 141.30 \pm 0.01 | 141.400 | 120 | \pm 10 | 109.80 | 1.69 | \pm 0.08 | 1.040 | 155 | 2 | | |
| 143.75 \pm 0.01 | 143.610 | 130 | \pm 30 | 88.00 | 60 | \pm 10 | 60.000 | 157 | 2 | | |
| 145.66 \pm 0.01 | 145.600 | 150 | \pm 20 | 109.80 | 6.5 | \pm 0.3 | 6.160 | 155 | 2 | | |
| 147.02 \pm 0.01 | 146.900 | 130 | \pm 10 | 109.80 | 5.3 | \pm 0.2 | 3.760 | 155 | 2 | | |
| 148.2 \pm 0.2 | 148.400 | 120 | \pm 20 | 88.00 | 46 | \pm 10 | 38.000 | 154 | $\frac{1}{2}$ | | |
| 148.4 \pm 0.3 | 148.200 | 110 | \pm 10 | 109.80 | 8.6 | \pm 0.9 | 9.600 | 155 | 2 | | |
| 148.55 \pm 0.05 | 148.310 | 140 | \pm 30 | 99.95 | 24 | \pm 1 | 24.000 | 157 | 1 | | |
| 149.53 \pm 0.03 | 149.600 | 110 | \pm 40 | 109.80 | 36 | \pm 2 | 33.333 | 155 | 1 | | |
| 150.37 \pm 0.04 | 150.200 | 110 | \pm 40 | 109.80 | 80 | \pm 30 | 24.800 | 155 | 2 | | |
| 150.62 \pm 0.03 | 151.200 | 80 | \pm 30 | 86.00 | 23 | \pm 7 | 41.700 | 156 | $\frac{1}{2}$ | | |
| 152.27 \pm 0.01 | 152.200 | 150 | \pm 40 | 109.80 | 6.2 | \pm 0.8 | 8.000 | 155 | 1 | | |
| 153.80 \pm 0.05 | 154.000 | 160 | \pm 30 | 109.80 | 1.1 | \pm 0.2 | 1.120 | 155 | 2 | | |
| 156.4 \pm 0.1 | 156.300 | 110 | \pm 80 | 109.80 | 30 | \pm 10 | 7.680 | 155 | 2 | | |
| 156.70 \pm 0.02 | 156.430 | 140 | \pm 50 | 91.00 | 13 | \pm 5 | 19.760 | 157 | 2 | | |
| 160.00 | 160.000 | 58.6 | | 58.60 | 2.83 | | 2.830 | 152 | $\frac{1}{2}$ | | |
| 160.03 \pm 0.07 | 160.100 | 110 | \pm 50 | 109.80 | 10.3 | \pm 0.5 | 9.600 | 155 | 2 | | |
| 161.57 \pm 0.08 | 161.600 | 150 | \pm 20 | 109.80 | 21.6 | \pm 0.8 | 20.000 | 155 | 2 | | |
| 164.8 \pm 0.2 | 164.500 | 98 | \pm 7 | 77.00 | 158 | \pm 2 | 105.000 | 154 | $\frac{1}{2}$ | | |
| 165.00 \pm 0.09 | 164.830 | 100 | \pm 80 | 100.00 | 23 | \pm 6 | 20.560 | 157 | 2 | | |
| 168.20 \pm 0.09 | 168.300 | 123 | \pm 6 | 109.80 | 31 | \pm 4 | 30.133 | 155 | 1 | | |
| 168.60 \pm 0.04 | 168.030 | 99.95 | | 99.95 | 3.333 | | 3.333 | 157 | 1 | | |
| 169.4 \pm 0.1 | 169.250 | 90 | \pm 10 | 99.95 | 3.4 | \pm 0.2 | 3.280 | 157 | 2 | | |
| 170.2 \pm 0.1 | 170.300 | 80 | \pm 30 | 109.80 | 8 | \pm 1 | 8.320 | 155 | 2 | | |
| 170.4 \pm 0.1 | 170.400 | 85 | \pm 9 | 88.00 | 4.9 | \pm 0.4 | 5.000 | 154 | $\frac{1}{2}$ | | |
| 171.2 \pm 0.2 | 171.250 | 100 | \pm 10 | 99.95 | 120 | \pm 40 | 44.000 | 157 | 1 | | |
| 171.6 \pm 0.1 | 171.400 | 110 | \pm 60 | 109.80 | 18 | \pm 1 | 9.200 | 155 | 2 | | |
| 173.5 \pm 0.1 | 173.500 | 110 | \pm 80 | 109.80 | 33 | \pm 2 | 32.800 | 155 | 2 | | |
| 173.80 | 173.800 | 30.1 | | 30.10 | 86 | | 86.000 | 152 | $\frac{1}{2}$ | | |
| 175.46 \pm 0.05 | 175.600 | 110 | \pm 40 | 109.80 | 4.2 | \pm 0.6 | 2.080 | 155 | 2 | | |

Table V (continued) Epithermal Results: Resonance Parameters

| Energy eV | Energy | | Γ_γ meV | ENDF meV | Γ_n (2ag Γ_n for unassigned) meV | Γ_n ENDF meV | ISO- TOPE J | |
|-------------------|------------|---------------|------------------------|-----------------|---|---------------------------|-------------------|---------------|
| | ENDF eV | meV | | | | | ENDF meV | ENDF meV |
| 177.99 \pm 0.02 | 178.000 | 130 \pm 10 | 109.80 | 13 \pm 2 | 9.733 | 155 | 1 | |
| 178.73 \pm 0.03 | 178.550 | 140 \pm 20 | 145.00 | 17.0 \pm 1.0 | 16.000 | 157 | 2 | |
| 180.34 \pm 0.04 | 180.400 | 110 \pm 40 | 109.80 | 9.7 \pm 0.3 | 14.667 | 155 | 1 | |
| 183.20 \pm 0.05 | NEW | 110 \pm 40 | NEW | 1.3 \pm 0.2 | NEW | | | UNASSIGNED |
| 183.94 \pm 0.07 | 183.830 | 100 \pm 90 | 99.95 | 34 \pm 8 | 17.600 | 157 | 2 | |
| 185.11 \pm 0.04 | NEW | 110 \pm 60 | NEW | 0.6 \pm 0.1 | NEW | | | UNASSIGNED |
| 185.70 | 185.700 | 52.5 | 52.50 | 84 | | 84.000 | 152 | $\frac{1}{2}$ |
| 187.36 \pm 0.07 | NEW | 100 \pm 100 | NEW | 3.5 \pm 0.2 | NEW | | | UNASSIGNED |
| 189.30 \pm 0.06 | NEW | 100 \pm 80 | NEW | 0.3 \pm 0.1 | NEW | | | UNASSIGNED |
| 190.9 \pm 0.1 | 190.730 | 100 \pm 90 | 99.95 | 60 \pm 60 | 28.000 | 157 | 1 | |
| 194.6 \pm 0.1 | 194.530 | 110 \pm 50 | 99.95 | 60 \pm 80 | 44.800 | 157 | 2 | |
| 198.4 \pm 0.2 | 198.100 | 92 \pm 4 | 86.00 | 200 \pm 100 | 270.000 | 156 | $\frac{1}{2}$ | |
| 199.5 \pm 0.2 | 201.600 | 60 \pm 40 | 88.00 | 80 \pm 50 | 11.700 | 154 | $\frac{1}{2}$ | |
| DISCARDED | 201.600 | | 86.00 | | | 17.000 | 156 | $\frac{1}{2}$ |
| 201.99 \pm 0.01 | 202.100 | 160 \pm 40 | 86.00 | 50 \pm 10 | 266.000 | 156 | $\frac{1}{2}$ | |
| DISCARDED | 202.740 | | 99.95 | | | 9.600 | 157 | 1 |
| 203.10 | 203.100 | 58.8 | 58.80 | 97 | | 97.000 | 152 | $\frac{1}{2}$ |
| 203.39 \pm 0.02 | NEW | 130 \pm 10 | NEW | 0.98 \pm 0.04 | NEW | | | UNASSIGNED |
| 205.75 \pm 0.04 | 205.350 | 110 \pm 10 | 99.95 | 2.0 \pm 0.1 | 0.976 | 157 | 2 | |
| DISCARDED | 206.900 | | 99.95 | | | 1.360 | 157 | 2 |
| DISCARDED | 207.700 | | 58.60 | | | 5.230 | 152 | $\frac{1}{2}$ |
| 207.77 \pm 0.04 | 207.810 | 150 \pm 20 | 114.00 | 110 \pm 30 | 108.000 | 157 | 2 | |
| 209.1 \pm 0.2 | NEW | 120 \pm 10 | NEW | 1.1 \pm 0.2 | NEW | | | UNASSIGNED |
| 210.32 \pm 0.01 | NEW | 140 \pm 20 | NEW | 2.78 \pm 0.06 | NEW | | | UNASSIGNED |
| 211.57 \pm 0.02 | 211.000 | 99 \pm 8 | 88.00 | 45 \pm 1 | 35.000 | 154 | $\frac{1}{2}$ | |
| 212.32 \pm 0.02 | NEW | 100 \pm 10 | NEW | 0.64 \pm 0.02 | NEW | | | UNASSIGNED |
| 213.68 \pm 0.02 | NEW | 102 \pm 10 | NEW | 1.02 \pm 0.03 | NEW | | | UNASSIGNED |
| 214.77 \pm 0.01 | NEW | 130 \pm 20 | NEW | 5.5 \pm 0.5 | NEW | | | UNASSIGNED |
| 217.23 \pm 0.01 | 217.150 | 121 \pm 9 | 99.95 | 19.9 \pm 0.9 | 8.000 | 157 | 1 | |
| 218.57 \pm 0.02 | NEW | 140 \pm 10 | NEW | 1.89 \pm 0.03 | NEW | | | UNASSIGNED |
| 220.24 \pm 0.08 | 220.900 | 150 \pm 20 | 99.95 | 8.3 \pm 0.4 | 4.000 | 157 | 1 | |
| 222.22 \pm 0.03 | 222.000 | 80 \pm 20 | 120.00 | 50 \pm 20 | 50.000 | 160 | $\frac{1}{2}$ | |
| 223.30 | 223.300 | 64.2 | 64.20 | 301 | | 301.000 | 152 | $\frac{1}{2}$ |
| 224.90 \pm 0.02 | 224.000 | 100 \pm 100 | 88.00 | 110 \pm 60 | 18.000 | 154 | $\frac{1}{2}$ | |
| 227.91 \pm 0.02 | 228.300 | 100 \pm 100 | 99.95 | 52 \pm 3 | 6.560 | 157 | 2 | |
| 229.52 \pm 0.02 | NEW | 100 \pm 70 | NEW | 9.7 \pm 0.5 | NEW | | | UNASSIGNED |
| 230.86 \pm 0.05 | NEW | 100 \pm 100 | NEW | 3.7 \pm 0.2 | NEW | | | UNASSIGNED |
| 231.40 | 231.400 | 62 | 62.00 | 46 | | 46.000 | 152 | $\frac{1}{2}$ |
| 232.85 \pm 0.01 | NEW | 100 \pm 90 | NEW | 2.2 \pm 0.2 | NEW | | | UNASSIGNED |
| 235.9 \pm 0.2 | NEW | 70 \pm 60 | NEW | 1.4 \pm 0.2 | NEW | | | UNASSIGNED |
| 237.3 \pm 0.1 | NEW | 100 \pm 100 | NEW | 5.8 \pm 0.2 | NEW | | | UNASSIGNED |
| 238.00 | 238.000 | 100 | 100.00 | 223.6 | | 223.600 | 152 | $\frac{1}{2}$ |
| 239.56 \pm 0.03 | 239.550 | 120 \pm 20 | 99.95 | 250 \pm 40 | 152.000 | 157 | 2 | |
| 243.17 \pm 0.01 | 242.700 | 90 \pm 20 | 105.00 | 50 \pm 20 | 60.000 | 158 | $\frac{1}{2}$ | |
| 245.16 \pm 0.02 | 244.000 | 98 \pm 9 | 86.00 | 3.25 \pm 0.06 | 3.100 | 156 | $\frac{1}{2}$ | |
| 246.80 \pm 0.01 | 244.600 | 118 \pm 9 | 99.95 | 19.8 \pm 0.5 | 4.400 | 157 | 1 | |
| 248.83 \pm 0.01 | 246.640 | 120 \pm 10 | 99.95 | 5.0 \pm 0.1 | 9.280 | 157 | 2 | |
| 250.51 \pm 0.02 | 250.200 | 130 \pm 10 | 99.95 | 8.2 \pm 0.2 | 5.733 | 157 | 1 | |
| 252.40 | 252.400 | 52.4 | 52.40 | 127 | | 127.000 | 152 | $\frac{1}{2}$ |
| 253.25 \pm 0.03 | 252.800 | 101 \pm 9 | 88.00 | 26 \pm 1 | 12.000 | 154 | $\frac{1}{2}$ | |
| 254.87 \pm 0.01 | 255.000 | 130 \pm 10 | 99.95 | 18.6 \pm 0.5 | 3.600 | 157 | 1 | |

Table V (continued) Epithermal Results: Resonance Parameters

| Energy eV | Energy | | Γ_γ meV | ENDF meV | Γ_n (2ag Γ_n for unassigned) meV | Γ_n ENDF meV | ISO- TOPE J | |
|--------------|------------|---------|------------------------|-------------|---|---------------------------|-------------------|-------------------|
| | ENDF eV | meV | | | | | ENDF meV | ENDF meV |
| 256.46 | \pm 0.06 | 255.200 | 101 | \pm 10 | 99.95 | 1.46 \pm 0.09 | 3.733 | 157 1 |
| 258.01 | \pm 0.01 | 257.500 | 91 | \pm 7 | 88.00 | 40 \pm 1 | 34.000 | 154 $\frac{1}{2}$ |
| 259.25 | \pm 0.02 | NEW | 102 | \pm 10 | NEW | 1.11 \pm 0.03 | NEW | UNASSIGNED |
| 260.53 | \pm 0.01 | 260.500 | 120 | \pm 10 | 99.95 | 31 \pm 3 | 21.867 | 157 1 |
| 262.56 | \pm 0.01 | NEW | 104 | \pm 10 | NEW | 0.96 \pm 0.02 | NEW | UNASSIGNED |
| 264.89 | \pm 0.01 | NEW | 110 | \pm 10 | NEW | 1.30 \pm 0.03 | NEW | UNASSIGNED |
| 266.05 | \pm 0.01 | 265.610 | 110 | \pm 10 | 99.95 | 7.9 \pm 0.2 | 6.400 | 157 2 |
| 268.47 | \pm 0.01 | 268.020 | 140 | \pm 20 | 99.95 | 17.0 \pm 0.9 | 10.480 | 157 2 |
| 269.57 | \pm 0.03 | 269.200 | 120 | \pm 20 | 88.00 | 50 \pm 10 | 28.000 | 154 $\frac{1}{2}$ |
| 272.36 | \pm 0.02 | NEW | 100 | \pm 60 | NEW | 1.3 \pm 0.1 | NEW | UNASSIGNED |
| 277.38 | \pm 0.06 | 277.200 | 100 | \pm 300 | 105.00 | 40 \pm 60 | 18.000 | 158 $\frac{1}{2}$ |
| 279.40 | \pm 0.03 | NEW | 98 | \pm 10 | NEW | 0.44 \pm 0.03 | NEW | UNASSIGNED |
| 282.60 | | 282.600 | 49.1 | | 49.10 | 145 | 145.000 | 152 $\frac{1}{2}$ |
| 282.28 | \pm 0.05 | 281.640 | 110 | \pm 100 | 99.95 | 70 \pm 30 | 38.400 | 157 2 |
| 284.2 | \pm 0.1 | NEW | 100 | \pm 30 | NEW | 2.1 \pm 0.2 | NEW | UNASSIGNED |
| 285.24 | \pm 0.05 | NEW | 150 | \pm 40 | NEW | 2.7 \pm 0.4 | NEW | UNASSIGNED |
| 287.89 | \pm 0.04 | 287.330 | 100 | \pm 50 | 99.95 | 25 \pm 3 | 14.240 | 157 2 |
| 288.99 | \pm 0.03 | NEW | 140 | \pm 30 | NEW | 2.3 \pm 0.3 | NEW | UNASSIGNED |
| 291.08 | \pm 0.03 | 290.770 | 100 | \pm 50 | 99.95 | 51 \pm 9 | 65.333 | 157 1 |
| 292.37 | \pm 0.07 | NEW | 130 | \pm 30 | NEW | 2.2 \pm 0.2 | NEW | UNASSIGNED |
| 293.40 | | 293.400 | 71 | | 71.00 | 352 | 352.000 | 152 $\frac{1}{2}$ |
| 294.16 | \pm 0.01 | 293.700 | 130 | \pm 30 | 99.95 | 49 \pm 8 | 36.800 | 157 2 |
| 295.79 | \pm 0.08 | NEW | 100 | \pm 10 | NEW | 0.5 \pm 0.2 | NEW | UNASSIGNED |
| 298.0 | \pm 0.1 | NEW | 110 | \pm 10 | NEW | 0.38 \pm 0.08 | NEW | UNASSIGNED |

The resolved resonance energy region for ^{155}Gd in the ENDF/B-VI evaluation ends at 180 eV. As a result, fitting data above 180 eV was performed without initial estimates for resonance locations and widths, a challenging task.

Finally, if a resonance is clearly observed in both transmission and capture it has been added to the database shown in Table V. In these cases, the isotope and spin are listed as unassigned and their associated neutron widths are given as $2ag\Gamma_n$ where ‘a’ is abundance and ‘g’ is the statistical weighting factor, $g = (2J+1) / [2(2I+1)]$, where I is the spin of the target nucleus and J is the total angular momentum of the compound state (also known as the spin state of the resonance) in units of $\hbar/2\pi$ where \hbar is Plank’s constant.

An example of the detailed descriptions available for the entire epithermal region in Reference 1 is repeated here for the 200-225 eV region. Resonances in this region are shown in Figure 5. Four resonances from ENDF have been excluded from the present analysis; 201.6 eV in ^{156}Gd , 202.74 eV in ^{157}Gd , 206.9 eV in ^{157}Gd , and 207.7 eV in ^{152}Gd . There are two reasons for these omissions. First, no author has explicitly seen any of these four resonances. Second, inclusion of these resonances does not improve the fit to the data.

There are four resonances listed in ENDF in the 201-203 eV region. The first of these, at 201.6 eV in ^{154}Gd was identified by Reference 7. It has been moved to 199.4 eV in the present fit. The next two resonances, 201.6 eV in ^{156}Gd and 202.1 eV in ^{156}Gd , have never both been observed. Mughabghab and Chrien⁴ and Coceva and Stefanon²⁹ each saw a single resonance at 202.1 and 201.8 eV, respectively. However, two resonances are listed in Reference 27 and in ENDF. Only one resonance is listed at 202 eV in ^{156}Gd in the present analysis. Another specific omission of a resonance listed in ENDF occurred at 206.9 eV in ^{157}Gd . This resonance is small in ENDF, $\Gamma_n = 1.36$ meV, and cannot be traced to any of the Gd experiments discussed in this report. It does not improve the fit and has been omitted from the present results. ENDF contains a ^{152}Gd resonance at 207.7 eV, but a review of the literature failed to reveal the source of this resonance. While, in general, ^{152}Gd resonances were not varied, this particular resonance was omitted from the present analysis. The effect of removing this resonance on the widths of the nearest resonance at 207.8 eV is negligible.

Seven new resonances have been added in the 200-225 eV region. The first, at 203.1 eV, is a shoulder on the 202 eV resonance in ^{156}Gd (see Figure 5). A new resonance has been proposed at 209.1 eV. It is a shoulder on the larger 207.77 eV resonance in ^{157}Gd . Five more resonances have been assigned at 210.32, 212.32, 213.68, 214.77, and 218.57 eV to account for structure apparent in the data in Figure 5.

VI.B.3 Results- Epithermal; Justification for New Resonances

Figure 6 shows a ‘staircase’ plot of gadolinium level density including all new resonances added during the present analysis. The plot of observed levels vs energy shows a good fit to a straight line which agrees with the statistical model of the nucleus up to about 50 eV. All levels are s-wave. Elemental gadolinium is shown because there is no assignment of isotope to the proposed new resonances. Above 50 eV a significant number of levels are missed. Therefore, even with the resonances added in the present analysis, the expectation of constant level density vs energy is not exceeded.

VI.C Results- Resonance Integrals and Thermal Cross Sections

Thermal cross sections and infinitely dilute capture resonance integrals (RI) have been calculated using ENDF and RPI resonance parameters. The isotopic ENDF evaluations used are from ENDF/B-VI updated through release 8. These files were processed using NJOY²⁸ into pointwise (Energy, cross section) data and isotopic thermal (2200 m/s) cross sections were obtained. The original ENDF files were then modified by replacing the original File 2 resonance parameters with those determined in the present work for all resonances below 300 eV. All resonances listed in Table IV and Table V, except those designated “UNASSIGNED” in those tables, were included. The resulting modified-ENDF files were processed using NJOY²⁸ and thermal cross sections and resonance integrals were obtained.

Thermal cross sections from the present measurements are compared to those of ENDF in Table VI and Table VII. The units of all cross sections in the tables are barns. The units of abundance are percent. The most significant departure of the present results from ENDF thermal capture cross sections is in ^{157}Gd . This 11% reduction (from 254000 barns for ENDF to 226000 barns for RPI) is consistent with the \approx 9% reduction in neutron width for the thermal ^{157}Gd resonance (see Table IV). An insignificant reduction in thermal capture cross section is seen in ^{155}Gd . This is due to the competing effects of a 7% reduction in neutron width compensated by a 3.7% reduction in total width ($\Gamma_n + \Gamma_\gamma$) and an energy shift toward the thermal energy (0.0253 eV) point. The thermal capture cross section of elemental gadolinium is \approx 9% lower than that calculated from ENDF parameters.

A significant reduction of thermal elastic cross section (Table VII) of the present results from ENDF occurs in ^{157}Gd (from 1010 to 798 barns). Thermal elastic scattering cross sections are proportional to Γ_n^2 . So, the reduction in thermal elastic cross section of ^{157}Gd is consistent with the \approx 9% reduction in neutron width for the thermal ^{157}Gd resonance (see Table IV). Thermal elastic scattering cross section for ^{157}Gd has a large uncertainty since it is essentially the small difference of two large numbers (total and capture cross sections). ^{156}Gd also exhibits a large deviation from ENDF in its small and statistically uncertain thermal elastic cross section. ^{156}Gd has only 2 resonances below 100 eV. The increase in its thermal elastic cross section is due to the substantial increase in the neutron width of the 80 eV resonance (see Table V). However, the uncertainty on that neutron width (see Table V) encompasses the majority of the increase.

Resonance integrals (Table VIII) are given for each isotope as well as their contribution to the elemental values. The integrations extend from 0.5 eV to 20 MeV. The low energy cutoff is above the thermal region doublet. The elemental resonance integral for Gd as measured is 2.8% (11 b) larger than that of ENDF. The largest fractional increases in isotopic contributions occur in ^{154}Gd and ^{158}Gd . ^{154}Gd and ^{158}Gd have far fewer resonances than ^{155}Gd or ^{157}Gd . A 14% increase in ^{158}Gd resonance integral compared to ENDF was measured. This is dominated by the 22.3 eV resonance whose neutron width changed by approximately the same amount. The resonance integral of ^{154}Gd is 20% larger than that calculated from ENDF resonance parameters. The ^{154}Gd resonance integral is larger than ENDF due to larger widths for resonances at 22.5, 49.63, 65.21, and 76.00 eV (see Table V). ^{155}Gd contributes more than half of the elemental Gd capture resonance integral and its contribution is virtually unchanged when compared to that calculated from ENDF parameters.

Table VI - Thermal capture cross sections. A comparison of ENDF/B-VI to RPI results. Cross section units are barns. The units of abundance are percent.

| Thermal Capture Cross Sections | | | | | | | |
|--------------------------------|-------|-----------------|---------------------------|----------|-----------------|---------------------------|----------|
| Isotope | Abund | ENDF | | | RPI | | |
| | | Thermal Capture | Contribution to Elemental | Percent | Thermal Capture | Contribution to Elemental | Percent |
| Gd152 | 0.200 | 1050. | 2.10 | 0.00430 | 1050. | 2.10 | 0.00430 |
| Gd154 | 2.18 | 85.0 | 1.85 | 0.00379 | 85.8 | 1.87 | 0.00422 |
| Gd155 | 14.80 | 60700. | 8980. | 18.4 | 60200. | 8910. | 20.1 |
| Gd156 | 20.47 | 1.71 | 0.350 | 0.000717 | 1.74 | 0.356 | 0.000804 |
| Gd157 | 15.65 | 254000. | 39800. | 81.6 | 226000. | 35400. | 79.9 |
| Gd158 | 24.84 | 2.01 | 0.499 | 0.00102 | 2.19 | 0.544 | 0.00122 |
| Gd160 | 21.86 | 0.765 | 0.167 | 0.000342 | 0.755 | 0.165 | 0.000372 |
| Gd | -- | | 48800. | 100.0 | | 44300. | 100.0 |

Table VII - Thermal elastic scattering cross sections. A comparison of ENDF/B-VI to RPI results. Cross section units are barns. The units of abundance are percent.

| Thermal Elastic Cross Sections | | | | | | | |
|--------------------------------|-------|-----------------|---------------------------|---------|-----------------|---------------------------|---------|
| Isotope | Abund | ENDF | | | RPI | | |
| | | Thermal Elastic | Contribution to Elemental | Percent | Thermal Elastic | Contribution to Elemental | Percent |
| Gd152 | 0.200 | 23.4 | 0.0468 | 0.0277 | 23.4 | 0.0468 | 0.0342 |
| Gd154 | 2.18 | 7.29 | 0.159 | 0.0941 | 6.69 | 0.146 | 0.107 |
| Gd155 | 14.80 | 60.8 | 8.99 | 5.32 | 59.7 | 8.84 | 6.45 |
| Gd156 | 20.47 | 5.64 | 1.16 | 0.686 | 6.93 | 1.42 | 1.04 |
| Gd157 | 15.65 | 1010. | 157. | 92.9 | 798. | 125. | 91.2 |
| Gd158 | 24.84 | 3.30 | 0.820 | 0.485 | 3.27 | 0.812 | 0.593 |
| Gd160 | 21.86 | 3.63 | 0.795 | 0.470 | 3.63 | 0.794 | 0.580 |
| Gd | -- | | 169. | 100.0 | | 137. | 100.0 |

Table VIII – Infinitely dilute neutron capture resonance integrals. A comparison of ENDF/B-VI to RPI results. Cross section units are barns. The units of abundance are percent.

| Capture Resonance Integral | | | | | | | |
|----------------------------|-------|------------|---------------------------|---------|------------|---------------------------|---------|
| Isotope | Abund | ENDF | | | RPI | | |
| | | Capture RI | Contribution to Elemental | Percent | Capture RI | Contribution to Elemental | Percent |
| Gd152 | 0.200 | 476. | 0.952 | 0.243 | 476. | 0.952 | 0.237 |
| Gd154 | 2.18 | 217. | 4.73 | 1.21 | 261. | 5.69 | 1.42 |
| Gd155 | 14.80 | 1540. | 228. | 58.3 | 1570. | 232. | 57.7 |
| Gd156 | 20.47 | 105. | 21.5 | 5.50 | 104. | 21.3 | 5.30 |
| Gd157 | 15.65 | 755. | 118. | 30.2 | 789. | 123. | 30.6 |
| Gd158 | 24.84 | 62.8 | 15.6 | 3.99 | 71.5 | 17.8 | 4.43 |
| Gd160 | 21.86 | 7.89 | 1.72 | 0.440 | 7.66 | 1.68 | 0.418 |
| Gd | -- | | 391. | 100. | | 402. | 100. |

VII. Discussion- Uncertainties

In Table IV and Table V, estimated uncertainties (on the order of 1σ) are given for the present measurements. They are based upon an envelope of plausible values representing the differences between data sets of equal quality. The sensitivity of the resonance parameters resulting from SAMMY fits to different subsets of the overall data was the method used to estimate the uncertainty on the resultant parameters.

In the thermal region these sensitivity calculations, used to define the uncertainties on resonance parameters in the thermal region, consisted of:

- 1) Uncertainty associated with the balance of interactions between ^{155}Gd and ^{157}Gd
- 2) Consistency among natural metal samples of various thickness
- 3) Consistency within transmission data within the same experiment
- 4) Uncertainty in capture flux normalization
- 5) Experimental reproducibility of transmission results.

In the epithermal region, uncertainties on resonance parameters include:

- 1) Consistency between capture and transmission results
- 2) Stability of radiation widths
- 3) Uncertainty associated with the transmission background
- 4) Bayesian statistical errors calculated by the SAMMY program

A detailed discussion of the uncertainty analysis in the present work is given in Reference 1. The variability of the results is most likely due to systematic errors.

A systematic error is a bias, rather than a random error, and may be due to features which are common to both capture and transmission measurements. The transmission and capture measurements are independent and complementary methods for determining resonance parameters. Features common to both types of experiments and possible sources of systematic uncertainties include using the same electron accelerator, the same neutron-producing target, the same method for determining flight path length, some of the same Gd samples, and some of the same data acquisition electronics. Other potential sources of error include capture flux normalization and the analytical descriptions of the resolution functions.

Uncertainties in sample thickness given in Table III are not included in the final uncertainties given in Table IV and Table V.

VIII. Conclusions

Resonance parameters were extracted from combined capture and transmission data sets using the multi-level R-matrix Bayesian code SAMMY. The analysis included Doppler broadening, resolution broadening and multiple scattering correcting of capture data. Separate resolution functions for transmission and capture were used.

The present measurements assumed the same spin assignments as ENDF for all resonances analyzed.

Neutron widths (Table IV) and thermal (2200 m/s) capture cross sections (Table VI) of the thermal doublet are smaller than currently published (ENDF) values. The neutron widths in particular are significantly smaller than those of ENDF. The thermal (2200 m/s) cross section of ^{157}Gd is 11% smaller than that of ENDF.

In the epithermal region, a great deal of improvement has been made to the Gd resonance parameter database. In the energy region near 96 eV, and particularly above 165 eV, significant changes are suggested to ENDF parameters. New resonances have been suggested where comparisons of data to calculations clearly show they are needed.

Any future gadolinium measurement must be improved beyond the current methods. There were internal inconsistencies between thermal transmission and capture results. There were internal inconsistencies within thermal transmission measurements. The magnitude of these inconsistencies was quantified by the uncertainties on the resonance parameters quoted in Table IV.

Results in the epithermal region could be improved with the use of separated isotopes. Samples would need to be thicker for this region than the samples produced for use in the present measurement in the thermal region. That is, grams of separated isotopes would be needed for epithermal measurements.

IX. References

1. G. LEINWEBER, D. P. BARRY, M. J. TRBOVICH, J. A. BURKE, N. J. DRINDAK, H. D. KNOX, R. V. BALLAD, R. C. BLOCK, Y. DANON, and L. I. SEVERNIAK, "Neutron Capture and Transmission Measurements and Resonance Parameter Analysis of Gadolinium," DOE Office of Scientific and Technical Information, OSTI ID: To Be Determined, (2005).
2. P. F. ROSE and C. L. DUNFORD, "ENDF-102 Data Formats and Procedures for the Evaluated Nuclear Data File ENDF-6," BNL-NCS-44945, Rev. 2, Brookhaven National Laboratory (1997).
3. H. BJERRUM MØLLER, F. J. SHORE, and V. L. SAILOR, "Low-Energy Neutron Resonances in Erbium and Gadolinium," *Nucl. Sci. Eng.*, **8**, 183-192 (1960).
4. S.F. MUGHABGHAB and R. E. CHRIEN, "S-Wave Neutron Strength Functions of the Gd Isotopes," *Phys. Rev.* **180**, 1131-1138 (1969).
5. F. B. SIMPSON, "Neutron Resonance Parameters for Sm^{147} , Sm^{149} , Gd^{155} , and Gd^{157} ," *Bull. Am. Phys. Soc.*, **2**, 42(NA7) (1957).
6. M. P. FRICKE, W. M. LOPEZ, S. J. FRIESENHAHN, A. D. CARLSON, D. COSTELLO, "Neutron Resonance Parameters and Radiative Capture Cross Section of Gd from 3 eV to 750 keV," *Nucl. Phys. A*, **146**, 337-358 (1970).
7. F. RAHN, H. S. CAMARDA, G. HACKEN, W. W. HAVENS, JR., H. I. LIOU, and J. RAINWATER, "Neutron resonance spectroscopy: $^{154,158,160}\text{Gd}$," *Phys. Rev. C (Nucl. Phys.)*, **10**, 1904 (1974).
8. V. A. ANUFRIEV, S. I. BABICH, S. M. MASYONOV, (C, 87KIEV,2, 225, 8709) NNDC CINDA EXFOR ENTRY # 40984 (1987).
9. R. L. MACKLIN, "Neutron Capture Resonances of ^{152}Gd and ^{154}Gd ," *Nucl. Sci. Eng.*, **95**, 304-310 (1987).
10. F.N.BELYAEV,V.P.BOLOTSKIY,B.V.EFIMOV,G.N.MURADYAN, *Jour. Jaderaja Fizika* (YF,52,(3),625,9009) Engl transl. = SNP, Soviet Jour. of Nucl. Phys.
11. E. N. KARZHAVINA, NGUEN NGUEN PHONG, A.B. POPOV, *Jour. Jaderno-Fizicheskie-Issledovanija* (progress reports), (R,YFI-6,135,6811) (1968).
12. E.N.KARZHAVINA, KIM-SEK-SU, A. B. POPOV, *Joint Inst. For Nucl Res.*, Dubna. Reports, (R,JINR-P3-6948,73) (1973).
13. M. ASGHAR, P. ASGHAR, E. SILVER, J. TROCHON, *Nucl. Phys. A*, **145**, 549 (1970).

14. R. E. SLOVACEK, R. C. BLOCK, Y. DANON, C. WERNER, G.-U. YOUNK, J. A. BURKE, N. J. DRINDAK, F. FEINER, J. A. HELM, K. W. SEEMANN, "Neutron Cross-Section Measurements at the Rensselaer LINAC," Proc. Topl. Mtg. Advances in Reactor Physics, April 11-15, 1994, Knoxville, Tennessee

15. R. C. BLOCK, P. J. MARANO, N. J. DRINDAK, F. FEINER, K. W. SEEMANN, and R. E. SLOVACEK, "A Multiplicity Detector for Accurate Low-Energy Neutron Capture Measurements," Proc. Int. Conf. Nuclear Data for Science and Technology, May 30-June 3, 1988, Mito, Japan, p. 383.

16. R. C. BLOCK, Y. DANON, C. J. WERNER, G. YOUNK, J. A. BURKE, N. J. DRINDAK, F. FEINER, J. A. HELM, J. C. SAYRES, and K. W. SEEMANN, "Neutron Time-of-Flight Measurements at the Rensselaer LINAC," Proc. Int. Conf. Nuclear Data for Science and Technology, May 9-13, 1994, Gatlinburg, Tennessee, Vol. 1, p. 81, American Nuclear Society (1994).

17. M. E. OVERBERG, B. E. MORETTI, R. E. SLOVACEK, R. C. BLOCK, "Photoneutron Target Development for the RPI Linear Accelerator," *Nucl. Instrum. & Meth. Physics Research A*, **438**, 253 (1999).

18. Y. DANON, R. E. SLOVACEK, and R. C. BLOCK, "The Enhanced Thermal Neutron Target at the RPI LINAC," *Trans. Am. Nucl. Soc.*, **68**, 473 (1993).

19. Y. DANON, R. E. SLOVACEK, and R. C. BLOCK, "Design and Construction of a Thermal Neutron Target for the RPI LINAC," *Nucl. Instrum. & Methods Physics Research A*, **352**, 596 (1995).

20. E. M. BAUM, H. D. KNOX, and T. R. MILLER, "Chart of the Nuclides," 16th Edition, KAPL Inc. (2002).

21. Y. DANON and R. C. BLOCK, *Nucl. Instrum. & Methods Physics Research A*, **485**, 585 (2002).

22. G. LEINWEBER, J. A. BURKE, H. D. KNOX, N. J. DRINDAK, D. W. MESH, W. T. HAINES, R. V. BALLAD, R. C. BLOCK, R. E. SLOVACEK, C. J. WERNER, M. J. TRBOVICH, D. P. BARRY, T. SATO, "Neutron Capture and Transmission Measurements and Resonance Parameter Analysis of Samarium," *Nucl. Sci. Eng.*, **142**, 1 (2002).

23. G. LEINWEBER, J. A. BURKE, C. R. LUBITZ, H. D. KNOX, N. J. DRINDAK, R. C. BLOCK, R. E. SLOVACEK, C. J. WERNER, N. C. FRANCIS, Y. DANON, and B. E. MORETTI, "Neutron Capture and Total Cross Section Measurements and Resonance Parameter Analysis of Zirconium up to 2.5 keV," *Nucl. Sci. Eng.*, **134**, 50 (2000).

24. N. M. LARSON, "Updated Users' Guide for SAMMY: Multilevel R-Matrix Fits to Neutron Data Using Bayes' Equations," ORNL/TM-9179/R5, Lockheed Martin Energy Research Corp., Oak Ridge National Laboratory, (2000).
25. D. B. SYME, "The Black and White-Filter Method for Background Determination in Neutron Time-of-Flight Spectrometry," *Nucl. Instrum. and Methods*, **198**, 357 (1982).
26. J. F. BREISMEISTER, Ed., "MCNP – A General Monte Carlo N-Particle Transport Code, Version 5," Los Alamos National Laboratory Rep. LA-UR-03-1987, April 24, 2003.
27. V. McLANE, P. F. ROSE, and C. L. DUNFORD, *Neutron Cross Sections*, Vol. 2, Academic Press, New York (1988).
28. R. E. MacFARLANE and D. W. MUIR, "The NJOY Nuclear Data Processing System Version 91," LA-12740-M, Los Alamos National Laboratory (Oct. 1994).
29. C. COCEVA and M. STEFANON, *Nucl. Phys. A*, **315**, 1 (1979).

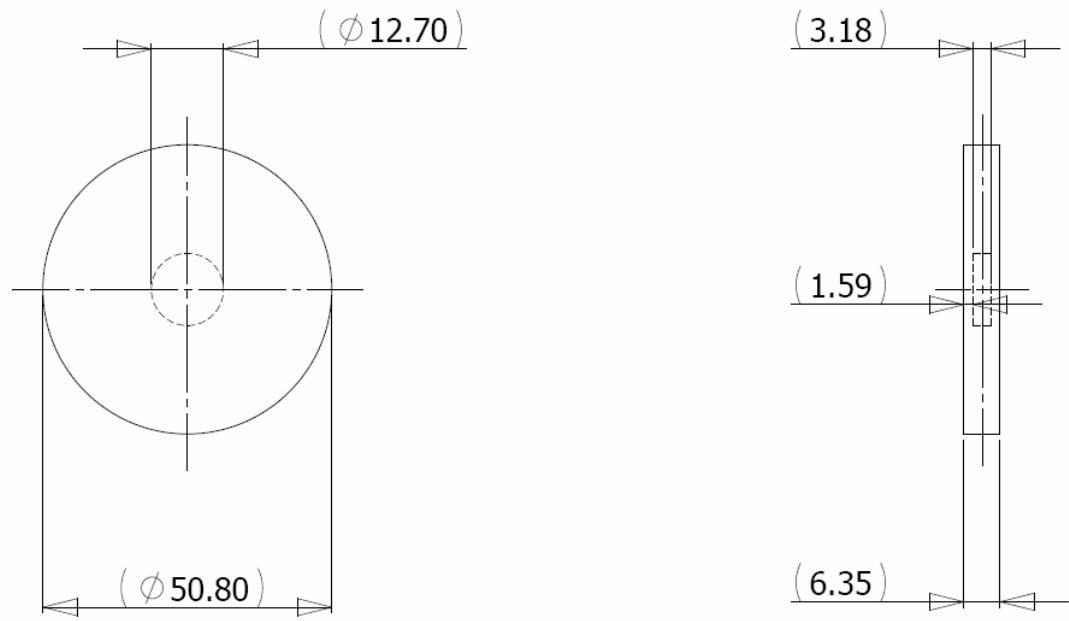


Figure 1- Geometry of the quartz cells used for liquid samples for thermal measurements. Units are mm.

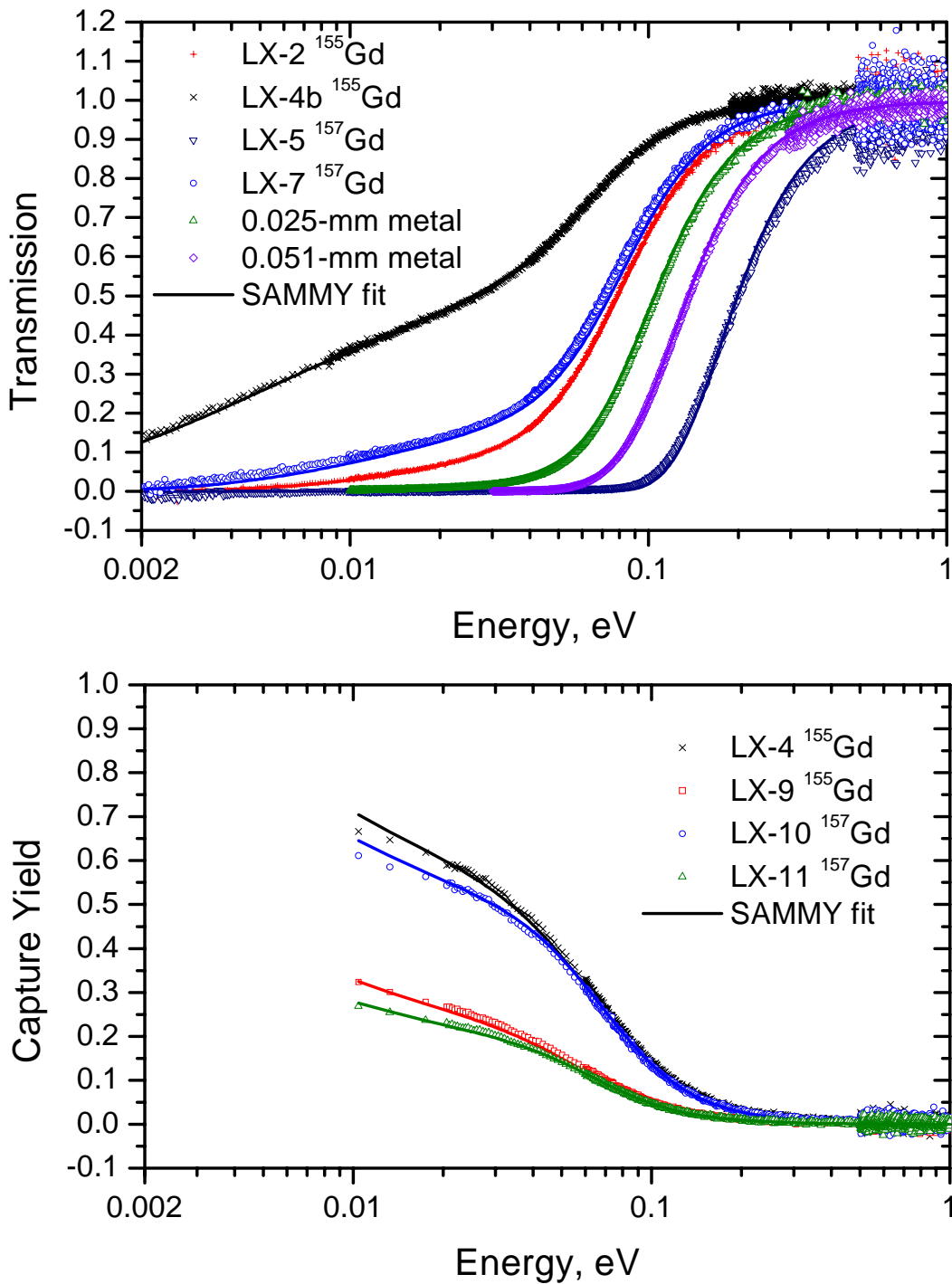


Figure 2 – An overview of transmission and capture data used in the thermal region and the SAMMY fits. The covariance matrix-linked fit represents the calculated transmissions and yields using RPI resonance parameters. Sample details are given in Tables II and III. “LX-4b” signifies data from sample LX-4 taken during the second thermal transmission experiment. Experimental details are given in Table I.

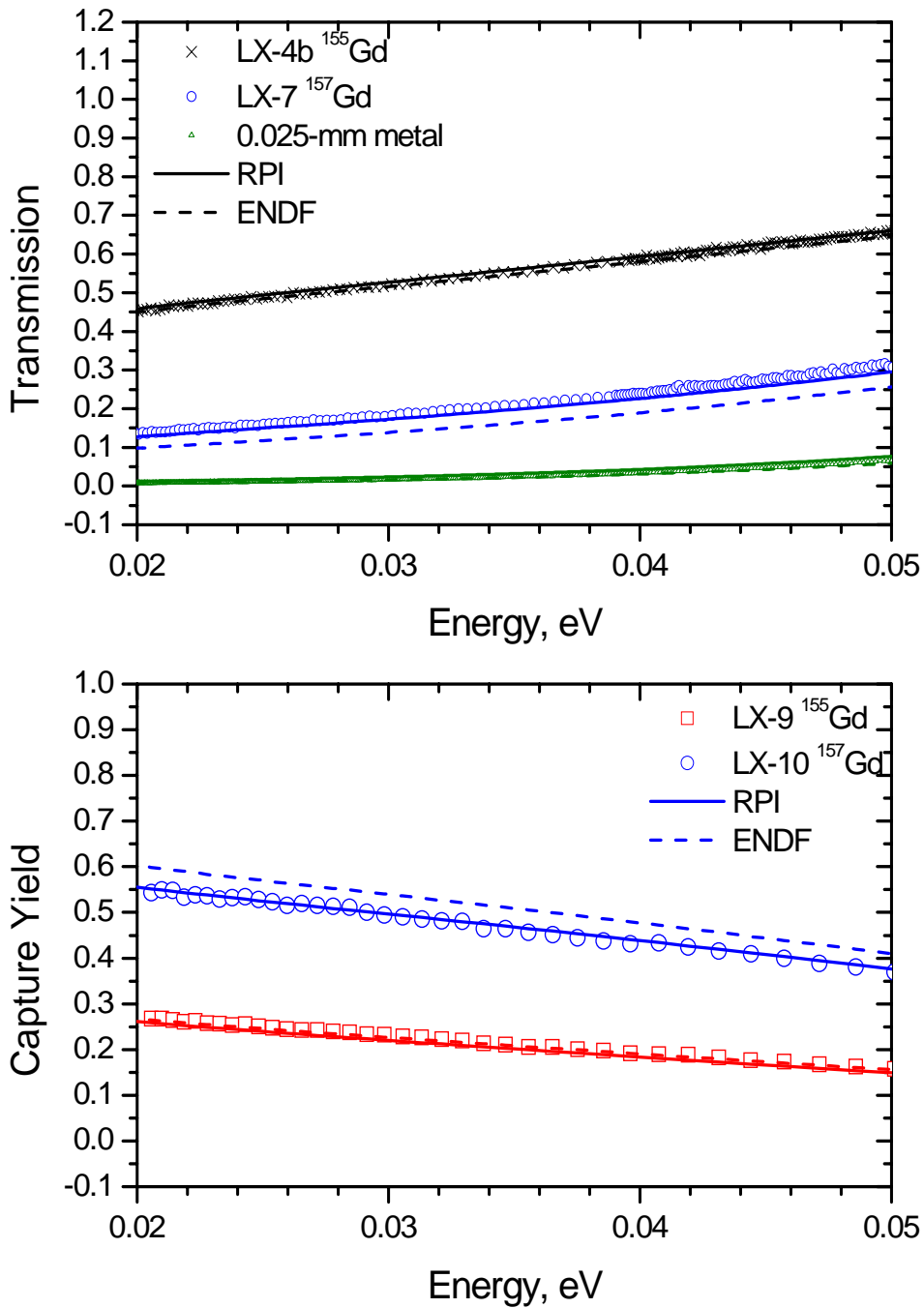


Figure 3 – Five thermal region sample's data, SAMMY fit and corresponding calculated transmissions and yields using ENDF resonance parameters. The thermal (0.0253 eV) capture cross section of ^{157}Gd was measured to be 9% lower than that of ENDF. The ^{155}Gd thermal capture cross section was not significantly different from ENDF. Sample details are given in Tables II and III. “LX-4b” signifies data from sample LX-4 taken during the second thermal transmission experiment. Experimental details are given in Table I.

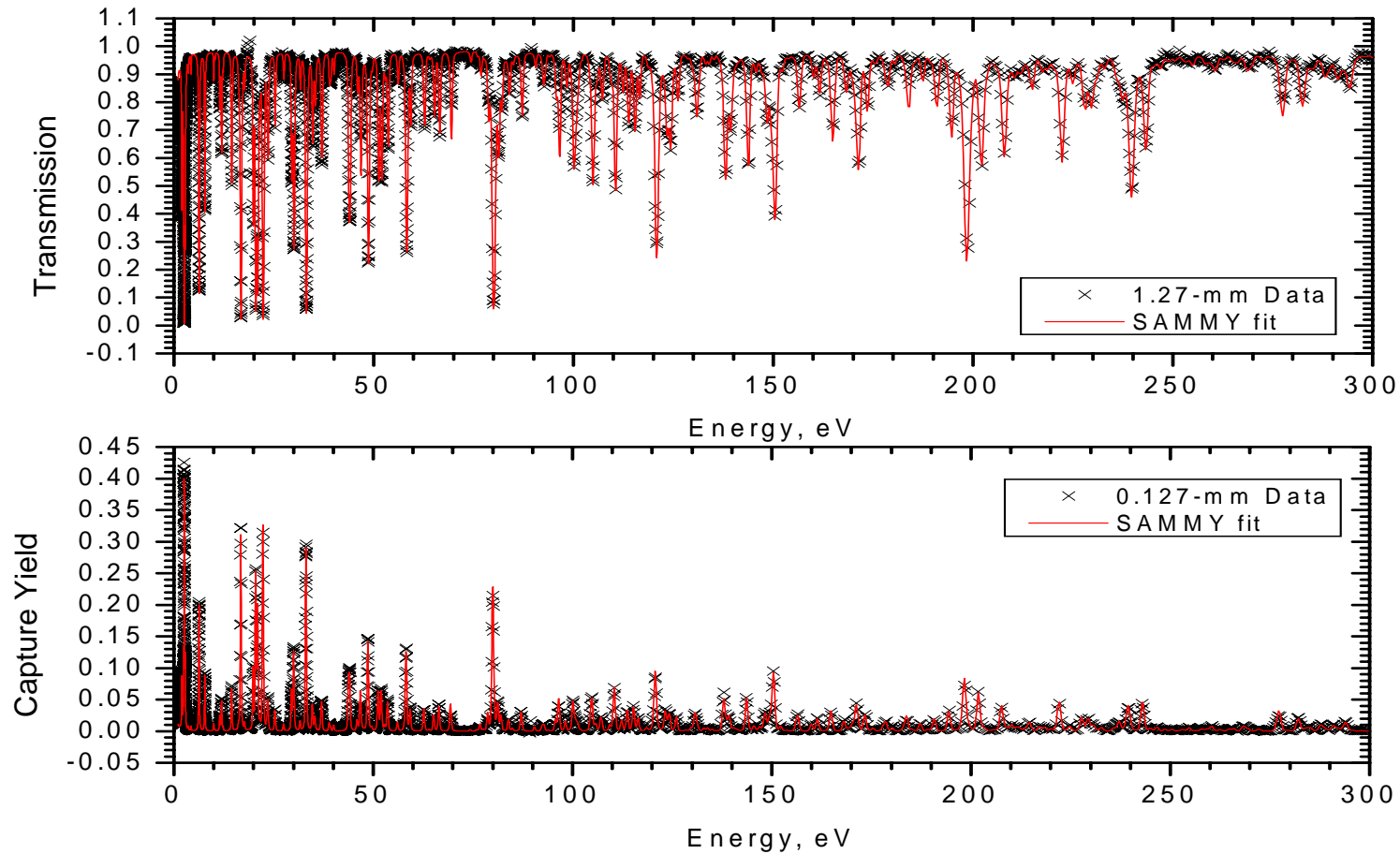


Figure 4 – An overview of the data and SAMMY fits in the epithermal region.

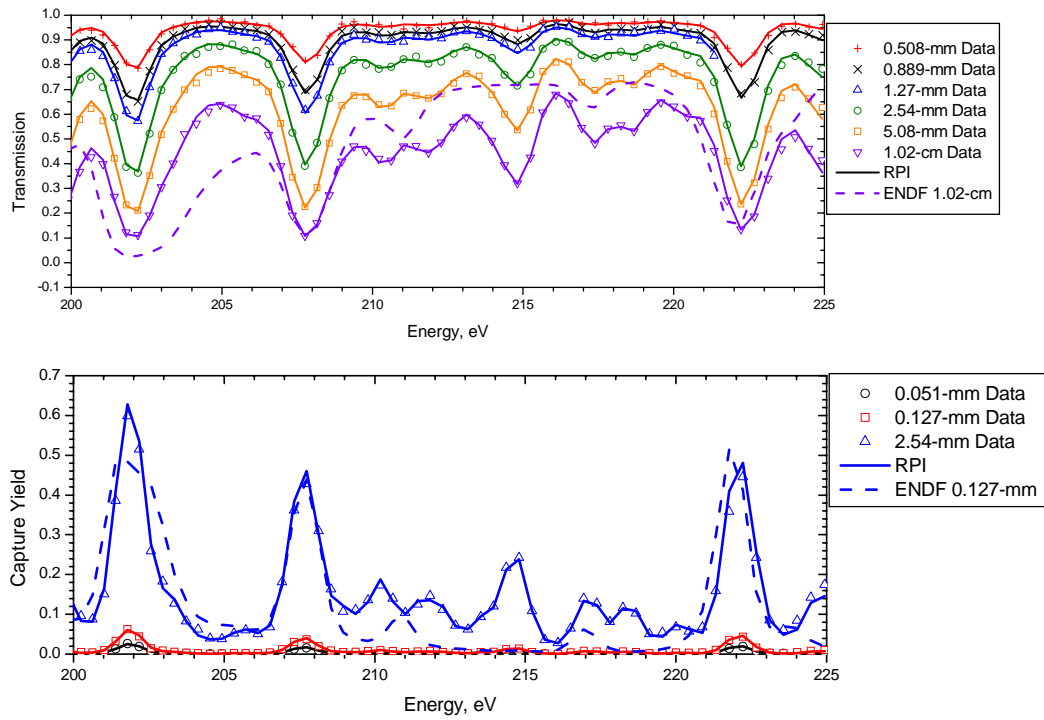


Figure 5 - An overview of transmission and capture data used in the 200-225 eV region and the SAMMY fits using the RPI parameters. The dashed lines represent the ENDF parameters for the thickest samples.

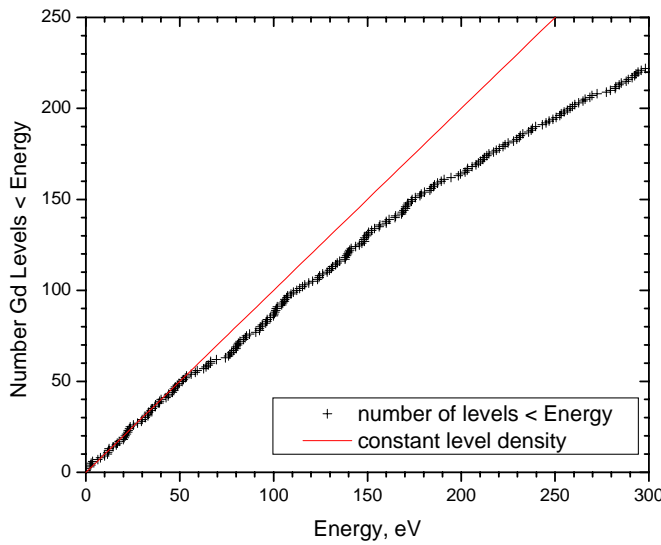


Figure 6 – ‘Staircase’ plot of elemental gadolinium observed levels vs energy shows a good fit to a straight line up to about 50 eV. Above 50 eV, even with the resonances added in the present analysis, the expectation of constant level density vs energy is not exceeded.